

1 ***A National Application of the Species Habitat Index for Ethiopia Reveals Uneven***
2 ***Habitat Change Across Plant Groups and Ecosystems***

3 *Moabe F. Fernandes*^{1*}, *Joseph White*¹, *Ermias Lulekal*², *Sebsebe Demissew*^{1,2}, *Jack F.*
4 *Plummer*¹, *Amy Barker*¹, *Shambel Alemu*², *Liz Brogan*¹, *Andrew Budden*¹, *Iain Darbyshire*¹,
5 *Becca Davis*¹, *Kelda F.V.A. Elliott*¹, *Tesfanesh Feseha*², *Bezawit Genanaw*², *Gabriella*
6 *Hoban*¹, *Hanny Lidetu*², *Lidet Mehari*², *Efrata Mekebib*³, *Henry Miller*¹, *Paloma Moore*¹,
7 *Lynda Murray*¹, *Sileshi Nemomissa*², *Tim Pearce*⁴, *Seth Ratcliffe*¹, *Alexandra Roberts*¹, *Harry*
8 *Smith*¹, *Vida J. Svahnström*^{1,5,6}, *Emily Terry*¹, *Jenna Willis*¹, *James Borrell*^{1,†}, *Steve*
9 *Bachman*^{1,†}, *Carolina Tovar*^{1,†}

10
11 **AFFILIATIONS**

12 1 – Royal Botanic Gardens, Kew, Richmond, TW9 3AE, United Kingdom

13 2 – Department of Plant Biology and Biodiversity Management, College of Natural and
14 Computational Sciences, The National Herbarium of Ethiopia, Addis Ababa University, Addis
15 Ababa, P.O. BOX 3434, Ethiopia

16 3 – Ethiopian Biodiversity Institute, Addis Ababa, P.O. BOX 30726, Ethiopia

17 4 – Royal Botanic Gardens, Kew Millennium Seed Bank, Wakehurst, Ardingly, West Sussex,
18 RH17 6TN, United Kingdom

19 5 – Science and Solutions for a Changing Planet DTP, The Grantham Institute, Imperial
20 College London, South Kensington, London, United Kingdom

21 6 – Department of Life Sciences, Imperial College London, Silwood Park, Ascot, Berkshire,
22 United Kingdom

23 * Corresponding Author: m.fernandes@kew.org

24 † Senior co-authorship

25
26 **ABSTRACT**

27 Accelerating delivery of the Kunming-Montreal Global Biodiversity Framework (GBF) requires
28 indicators that can detect species-level habitat change at policy-relevant scales. The Species
29 Habitat Index (SHI) offers a method to optimise resource allocation and enhance national
30 biodiversity reporting, but its broader utilisation has been constrained by significant data gaps,
31 particularly for taxa that are less well documented than birds and mammals. In this study, we

32 (i) examine how methodological choices impact the assessment of changes in species'
33 suitable habitat through the SHI, and (ii) develop a national SHI for plants of Ethiopia. We
34 compiled georeferenced occurrence records and IUCN-based habitat preferences for 1,247
35 plant species (141 families; 340 endemics) and combined these with a 29-year land-cover
36 time series (1992–2020) to quantify SHI. We first compared different geometry-based range-
37 mapping methods with species distribution models (SDMs) to assess their influence on SHI
38 estimates and then applied a combined approach to estimate national SHI trends for Ethiopian
39 plants. SHI trends were broadly robust across methods, with Rapoport's Mean Propinquity
40 polygons showing closest match with SDMs. Nationally, median SHI increased slightly
41 (+0.51%), but declines were common and disproportionately affected endemic and non-woody
42 species. Declines SHI trends were concentrated in species inhabiting shrubland and
43 grassland land-cover classes and were geographically clustered in highland regions
44 corresponding to the Afro-alpine and Dry Evergreen Afromontane Forest and Grassland
45 Complex vegetation types. These findings demonstrate that SHI can be applied to data-limited
46 floras using simplified range-mapping approaches, providing a scalable tool for biodiversity
47 monitoring. At the same time, the results highlight uneven responses to land-cover change
48 and the need to prioritise vulnerable ecosystems in Ethiopia's conservation planning.

49 **KEYWORDS**

50 Biodiversity indicators, Global Biodiversity Framework, Land-cover change, Monitoring,
51 Range-mapping, Plant conservation

52

53 **1 – INTRODUCTION**

54 Reversing current trends of biodiversity loss and environmental degradation requires a robust
55 monitoring framework supported by clear, precise, and reportable metrics and indicators, as
56 outlined in the Global Biodiversity Framework (GBF; CBD, Secretariat 2022). Metrics that
57 effectively incorporate environmental changes are essential for understanding the impacts of
58 habitat modification and conversion, the primary drivers of biodiversity loss (Díaz et al., 2019).
59 While these drivers have been relatively well-studied at the ecosystem level, particularly in
60 forests (e.g., Hansen et al., 2010; 2013), species-level habitat trends have received
61 comparatively less attention, despite their importance for assessing extinction risk and
62 informing conservation decision-making (IUCN, 2012a).

63 Developing informative species-level indicators necessitates addressing key challenges in
64 species range mapping, specifically in minimising commission errors—areas incorrectly
65 mapped as part of the species' distribution where the species is absent—and in consistently
66 delineating only the suitable areas for a species, such as those defined by habitat and

67 elevation preferences (Rondinini et al., 2006; Brooks et al., 2019). The Area of Habitat (AOH),
68 as defined by Brooks et al. (2019), represents the spatial extent of suitable habitat within the
69 geographic range of a species, providing a more ecologically relevant measure of habitat
70 availability by reducing commission errors. While AOH plays a critical role in linking habitat
71 characteristics with species-level assessments and enhancing mapping of at-risk biodiversity
72 (Lumbierres et al., 2021; 2022), it typically represents the best map possible at a single point
73 in time. The lack of a temporal dimension limits AOH's ability to track changes in the habitat
74 coverage and availability, and their consequent impacts on species.

75 Advancements in remotely-sensed land-cover datasets with long-term time series (e.g., Jung
76 et al., 2020; Harper et al., 2023) offer unprecedented opportunities to quantify changes in
77 species' habitats over time (Rondinini et al., 2011; Bird et al., 2012; Pettorelli et al., 2014;
78 Visconti et al., 2016). The Species Habitat Index (SHI), developed as part of the indicator
79 framework of the Group on Earth Observations Biodiversity Observation Network (GEO BON)
80 (<https://geobon.org/>; GEO BON 2015), integrates these data to estimate AOH over time,
81 facilitating temporal assessments of species' habitat coverage (Jetz et al., 2019; Powers &
82 Jetz, 2019; Simkin et al., 2022). As part of the suite of indicators supporting the GBF
83 monitoring framework (CBD Secretariat, 2021; 2022; Jetz et al., 2022), the SHI has been
84 integrated into the Map of Life (<https://mol.org/>), enabling the tracking of habitat changes over
85 the past ~20 years for several species (e.g., Jetz et al., 2012). Beyond retrospective analyses,
86 the SHI can be projected forward under different shared socioeconomic pathways (SSPs)
87 (Powers & Jetz, 2019; Simkin et al., 2022), allowing for assessments of the potential impacts
88 of future climate and land-use changes on biodiversity.

89 By providing high temporal and spatial resolution, the SHI offers key advantages over
90 traditional biodiversity indicators like the IUCN Red List Index (RLI, see Butchart et al., 2004),
91 which operates on relatively coarse temporal and spatial scales and may result in a lag before
92 status changes are detected (Tittensor et al., 2014). Furthermore, SHI's capacity to integrate
93 data from multiple species across taxonomic groups and geographic regions addresses
94 limitations of indicators such as the Living Planet Index (LPI), which lacks representation for
95 several groups such as invertebrates, plants, and fungi (Ledger et al., 2023). Additionally, its
96 applicability at the national level offers a locally relevant index that optimises resource
97 allocation and enhances national biodiversity reporting against global commitments.

98 Despite its potential, the SHI has primarily been applied to well-documented taxa such as
99 mammals and birds (Powers & Jetz, 2019; Simkin et al., 2022). Broader utilisation of the SHI
100 has been largely constrained by significant data gaps, particularly for understudied groups
101 such as plants, fungi, and invertebrates, which lack comprehensive range maps, habitat

102 preferences, and elevation data. For example, approaches for mapping plant distributions
103 typically include the use of coarse-scale polygons (e.g., World Geographic Scheme for
104 Recording Plant Distributions, Brummitt 2001) or collations of georeferenced occurrence data,
105 which can, in turn, be converted into polygons using geospatial techniques (Willis et al., 2003;
106 Moat, 2020). Georeferenced occurrences can also be integrated with environmental layers to
107 create statistically robust species distribution models (SDMs), providing spatially explicit
108 habitat suitability estimates (Phillips et al., 2006; Guisan et al., 2017; Borgelt et al., 2022). The
109 accuracy of the different methods depends on the data quality and assumptions underpinning
110 each approach, potentially affecting SHI calculations. Evaluating the impact of different
111 mapping techniques on SHI accuracy is therefore critical for extending its application to data-
112 limited taxa and regions.

113 This study estimates the SHI for plants in Ethiopia, a country characterised by high species
114 richness and significant conservation challenges (Myers et al., 2000; Mittermeier et al., 2005;
115 Dinerstein et al., 2017), that includes habitat fragmentation primarily driven by anthropogenic
116 land-use change (Figure 1; Nyssen et al., 2014; Tolessa et al., 2017). Ethiopia's ecological
117 heterogeneity, spanning from arid lowlands to Afroalpine zones (Mittermeier et al., 2005; Friis
118 et al., 2010; Dinerstein et al., 2017), means that species may experience habitat changes
119 across diverse environmental gradients, offering important context for interpreting SHI across
120 different ecological settings. With over 5,500 plant species and a substantial number of
121 endemic (Friis et al., 2005; Kelbessa & Demissew, 2014; Demissew et al., 2021) and/or
122 threatened species (Abro et al., 2024), Ethiopia is an ideal case study for evaluating the
123 applicability of SHI as a national-level index for plants. Developing a national-level SHI for
124 Ethiopia enables assessments of land-cover modification on species' suitable habitat and
125 supports conservation prioritisation and evidence-based policy decisions.

126 In this study, we first examine how methodological choices impact the assessment of changes
127 in species' suitable habitat through the SHI. Specifically, we employ an ensemble of range-
128 mapping methods using species occurrences, including simple geometry-based polygons
129 alongside SDMs, to evaluate whether these approaches yield consistent trends in SHI.
130 Second, we assess whether Ethiopian plant species have experienced net gains or losses in
131 suitable habitat over time, exploring how species' ecological attributes—endemicity and life
132 form—influence SHI trends. Third, we identify the habitats and administrative zones (woredas)
133 with the highest concentrations of species with declining SHI trends and interpret these
134 patterns in relation to the major vegetation systems of Ethiopia (Friis et al., 2010). This
135 provides an ecologically meaningful and spatially explicit basis for prioritising conservation
136 actions relevant to Ethiopian policymakers. Finally, we discuss the potential of the SHI to guide
137 conservation efforts, examining its utility as a key tool for advancing biodiversity conservation.

138

139 **2 – METHODS**

140 **2.1 – Conservation Assessment, Elevation and Habitat Preferences**

141 To establish a robust dataset for estimating the SHI for Ethiopian plants, we initially compiled
142 data for those species with extinction risk assessments published on the IUCN Red List of
143 Threatened Species (IUCN, 2024). These assessments provide detailed textual information
144 on elevation and habitat preferences, which are necessary for estimating SHI. Using the
145 advanced search of the IUCN Red List (IUCN, 2024; version 2024.1, accessed in July 2024),
146 we retrieved data for 1,236 plant species recorded in Ethiopia. To expand this dataset, we
147 incorporated species from ongoing Red List assessment efforts, including initiatives from the
148 Global Centre on Biodiversity for Climate (GCBC) queued for release in upcoming Red List
149 updates (E. Lulekal, S. Alemu & T.R. Pearce, unpublished). These efforts contributed 203
150 species to the dataset. After harmonising taxonomy using the package rWCVP (Brown et al.,
151 2023) and excluding species lacking habitat data, the final dataset comprised 1,247 species
152 spanning 141 families. This included 340 endemic species, representing approximately two
153 thirds of Ethiopia's endemics and one fifth of the country's total flora. Of these, 554 are
154 classified as woody (e.g., tree and shrubs) and 693 as non-woody (e.g., herbs, epiphytes,
155 succulents). In terms of conservation status, 935 species are assessed as non-threatened
156 (LC, NT), while 312 are assessed as threatened or data deficient (DD, VU, EN, CR).

157 To account for incomplete and inconsistent data, we assigned default values reflecting
158 Ethiopia's extremes (-115 m for the Danakil Depression and 4,530 m for the Semien
159 Mountains; Asefa et al., 2020) to 382 species (~30% of the total) with missing or ambiguous
160 elevation data (e.g., identical lower and upper limits). We addressed the lack of spatially
161 explicit, multi-year habitat classification datasets aligned with the IUCN Habitats Classification
162 Scheme (IUCN, 2012b) by utilising an expert-based conversion table (available as
163 supplementary material in Santini et al., 2019) to reclassify habitats into categories compatible
164 with the European Space Agency Climate Change Initiative (ESA-CCI) land-cover layers
165 (Harper et al., 2023). To reduce noise in SHI calculations, we excluded aquatic and marginal
166 habitats due to high inter-annual variability and retained only primary terrestrial habitats for
167 each species.

168

169 **2.2 – Occurrence Records**

170 Verified occurrence data from the IUCN Red List (IUCN, 2024) and unpublished Ethiopian
171 endemic species database (E. Lulekal, S. Alemu & T.R. Pearce, unpublished) were integrated

172 with data from multiple sources, including the Global Biodiversity Information Facility (GBIF;
173 <https://www.gbif.org/>), the Botanical Information and Ecology Network (BIEN;
174 <https://bien.nceas.ucsb.edu/bien/>), and RAINBIO (Dauby et al., 2016). All records were
175 consolidated using the bdc package (Ribeiro et al., 2022) and filtered to include only those
176 records collected from the year 1950 onwards within Africa. To ensure geospatial data quality,
177 we implemented a set of data cleaning procedures in the package CoordinateCleaner (Zizka
178 et al., 2019), removing records with potentially erroneous coordinates. This included removing
179 records that: (i) fell within country or province centroids; (ii) were located in capital cities or
180 near botanical institutes; (iii) had invalid or missing coordinates; or (iv) occurred along
181 coastlines. To further improve geospatial data quality, we performed a spatial thinning process
182 using the `occ_filt_geo` function from the `flexsdm` package (Velazco et al., 2022), thinning the
183 records to a minimum distance of 1 km between occurrences.

184

185 **2.3 – Elevation and Land-cover**

186 We obtained elevation data at a resolution of 30 arc-seconds (approximately 1 km² at the
187 equator) from the Shuttle Radar Topography Mission (SRTM) DEM Digital Elevation Database
188 of the Consortium for Spatial Information (CGIAR-CSI) using the `geodata` package (Hijmans
189 et al., 2023). Due to the lack of a spatially explicit habitat classification aligned with the IUCN
190 Habitats Classification Scheme (IUCN, 2012b) and suitable for calculating SHI over large time
191 scales—i.e., Jung et al.'s (2020) product only covers five years (2015—2019)—we utilised
192 land-cover data from the ESA-CCI. Available at a resolution of 10 arc-seconds (approximately
193 300 m; Harper et al., 2023), this dataset spans a period of 29 years (1992—2020), offering
194 the advantage of providing a long time series. To ensure spatial compatibility and preserve
195 accurate area calculations, all layers were projected to a Cylindrical Equal Area (CEA)
196 coordinate system centred on Ethiopia (latitude: 9°, longitude: 39°) and resampled to a 1 km
197 resolution using the nearest neighbour method in the `terra` package (Hijmans, 2023) in the R
198 statistical environment (R Core Team, 2025).

199

200 **2.4 – SHI Estimation**

201 To assess temporal changes in suitable habitat, we first estimated Area of Habitat (AOH) for
202 each species for every year from 1992 to 2020. We generated annual AOH maps by removing
203 raster cells coded with unsuitable habitats and elevations from species' range maps (Brooks
204 et al., 2019). This resulted in a series of 29 AOH maps per species, capturing interannual
205 variation in availability of suitable habitat. We then calculated the SHI as the percentage

206 change in AOH area over time within Ethiopia, relative to the baseline year 1992. For non-
207 endemic species, this SHI is analogous to the species stewardship metric, which represents
208 the proportion of global AOH for a species within a given country (GEO BON, 2015; Jetz et
209 al., 2012; 2019; Powers & Jetz, 2019). While the original SHI framework can incorporate
210 habitat connectivity (e.g., Jetz et al., 2012; GEO BON, 2015; CBD Secretariat, 2021), our
211 analysis focuses solely on the net change in AOH over time. This SHI workflow was used
212 across both the comparison of range-mapping methods (Section 2.5), and the national-scale
213 SHI estimation for the plants of Ethiopia (Section 2.6) and is summarised in Figure 2.

214

215 **2.5 – Testing Range-Mapping Methods for SHI**

216 Estimating SHI requires annual maps of a species' AOH, which are built upon defined spatial
217 range maps representing the potential extent of the species' distribution (Rondinini et al., 2006;
218 Brooks et al., 2019). While range maps for well-known groups such as birds and mammals
219 are often available through expert-drawn polygons (e.g., Powers & Jetz, 2019; Lumbierres et
220 al., 2022; Simkin et al., 2022), they are rarely available for plant species. Consequently, range
221 maps for plants must often be derived from occurrence record data using either statistical or
222 geometric approaches.

223 In this study, we used Species Distribution Models (SDMs) as the benchmark method for
224 generating species' range maps. By integrating bioclimatic and environmental variables,
225 SDMs can reduce commission (inclusion of unsuitable areas) and omission errors (exclusion
226 of suitable areas) more effectively than simpler geometry-based range-mapping methods
227 (Phillips et al., 2006; Guisan et al., 2017; Borgelt et al., 2022). We focused on a subset of 727
228 species with ten or more unique records after data cleaning (Section 2.2). This threshold aligns
229 with established recommendations for reliable SDMs (van Proosdij et al., 2016) and allowed
230 us to develop statistically robust models using MaxEnt, implemented via the SDMtune
231 package (Vignali et al., 2020). We converted continuous suitability outputs into binary
232 (presence/absence) maps using a True Skill Statistic (TSS) thresholding approach.
233 Subsequently, each SDM binary map was used to generate the annual AOH maps from which
234 SHI values were calculated, following the procedures described in Section 2.4.

235 Because SDMs are usually resource-intensive, we tested the performance of more accessible,
236 geometry-based range mapping methods that can be applied more broadly, especially for
237 understudied taxa like plants. These methods are relatively easy to implement and can be
238 largely automated using available spatial analysis tools (e.g., R packages such as sf, rCAT,
239 and terra), offering a scalable alternative for SHI assessments based on more complex
240 mapping methods. We compared SHI trends derived from five alternative range-mapping

241 methods against those derived from benchmark SDMs (Supplementary Figure S1). The five
242 geometry-based methods, representing varying levels of omission and commission errors,
243 included: (i) convex hull (C-hull), defined as the minimum polygon enclosing all occurrence
244 points; (ii) alpha hull (A-hull), a non-convex polygon that considers spatial density of points;
245 (iii) 10 km buffer (Buffer), creating a 10 km radius area surrounding each point; (iv) Rapoport's
246 Mean Proximity polygons (Rapo), which subdivides subpopulations based on interpoint
247 distances derived from a minimum spanning tree (Rapoport, 1982; Willis et al., 2003); and (v)
248 a country-wide range (Country) that spans the whole extension of Ethiopia for all species. All
249 geometry-based species range maps were generated using the R packages *sf* (Pebesma,
250 2018; Pebesma & Bivand, 2023) and *rCAT* (Moat, 2020) and were rasterized to a 1 km
251 resolution using the *terra* package (Hijmans, 2023). We then applied the same SHI workflow
252 as with SDMs (described in Section 2.4 and illustrated in Figure 2) for each species across all
253 range-mapping methods.

254 To quantify the extent to which geometry-based range-mapping methods approximate SHI
255 trends derived from the benchmark SDMs, we calculated Pearson and Spearman correlation
256 coefficients based on the 29 annual AOH values for each species and method. These metrics
257 provide complementary insights into the agreement between methods; while Pearson
258 assesses the strength of the linear relationship and is sensitive to absolute differences in SHI
259 magnitude, Spearman assesses whether the relative ordering of values is preserved over
260 time. Additionally, we calculated Root Mean Square Error (RMSE) and Mean Square Error
261 (MSE) to quantify the average deviation between SHI values derived from geometry-based
262 methods and SDMs. To account for the multi-temporal nature of SHI and reduce the influence
263 of heterogeneous species trends, we calculated correlation and error metrics per species and
264 averaged them across mapping methods. Species with less than 10 km² of suitable habitat in
265 1992 (265 species, or 36.5% of the total) were excluded to reduce the influence of unrealistic
266 percentage changes resulting from very small initial AOH values. Correlation coefficients were
267 calculated using the *cor* function in base R (R Core Team, 2025), while RMSE and MSE were
268 calculated using the *Metrics* package (Hamner & Frasco, 2018).

269

270 **2.6 – National SHI Estimation**

271 To assess national level SHI trends for the flora of Ethiopia, we analysed a dataset of 1,247
272 species, combining SDMs and geometry-based methods. For the 727 species with 10 or more
273 occurrence records, we used the SDMs described above. For the remaining 520 species,
274 range maps were developed using Rapo, the best-performing polygon method based on
275 results from the subset analysis (see Section 3.1). For species with only one or two records

276 (61 species), we created 10 km buffer polygons around occurrence records. This approach
277 facilitated the inclusion of species lacking sufficient data for SDM generation, increasing the
278 national SHI coverage. For all species, SHI was calculated following the procedure described
279 in Section 2.4.

280 To explore how ecological characteristics influence trends in habitat suitability, we tested
281 whether SHI trends varied by biogeographical status (endemic vs. non-endemic) and
282 functional group (woody vs. non-woody) using a two-step analysis. We first evaluated temporal
283 trends in SHI by fitting simple linear regressions independently for each species, utilising the
284 percentage of change as the response variable and year as the predictor. The resulting slope
285 coefficients reflected the direction and magnitude of habitat change over time. In the second
286 step, we used these species-level SHI slopes as the response variable in a linear model, with
287 biogeographical status and functional group included as independent variables. All analyses
288 were conducted using the stats package in the R statistical environment (R Core Team, 2025).

289

290 **2.7 – Identifying Conservation Priorities through SHI Trends**

291 To identify priority habitats and regions for plant conservation in Ethiopia, we analysed the
292 ecological and spatial distribution of species with declining SHI trends. Based on species-
293 specific SHI trends (Section 2.6), we classified species as either declining (negative slope) or
294 non-declining (including both stable and increasing trends). To explore whether these two
295 groups are associated with distinct sets of habitats, we constructed a binary species × land-
296 cover matrix using ESA-CCI land-cover profiles. We employed a Non-Metric Multidimensional
297 Scaling (NMDS) with Jaccard dissimilarity to ordinate species into a reduced habitat space,
298 followed by a Permutational Analysis of Variance (PERMANOVA) to test whether declining
299 and non-declining species exhibit significantly different associations with ESA-CCI land-cover
300 classes. To identify which land-cover classes most strongly shaped differences between these
301 groups, we used the envfit function to fit habitat vectors to the NMDS ordination and conducted
302 a Similarity Percentage (SIMPER) analysis to quantify the relative contributions of individual
303 ESA-CCI land-cover classes to the observed dissimilarities. All these analyses were
304 conducted using functions from the vegan package (Oksanen et al., 2025).

305 In parallel, we conducted spatial analysis to identify Ethiopia's administrative zones with high
306 conservation importance based on SHI trends. For each zone, we quantified the number of
307 species with declining SHI trends by overlaying species' annual AOH maps with the woredas
308 (third level administrative units) obtained *via* the geoBoundaries package (Runfola et al.,
309 2020). A species was considered as present if any portion of its AOH intersected the zone in
310 any year from 1992 to 2020. To classify zones according to conservation priority, we ranked

311 zones into five equal-size categories (quintiles) using the `ntile()` function from the `dplyr`
312 package (Wickham et al., 2023), ranging from Very Low to Very High priority. This analysis
313 was conducted separately for all species, endemic species, and non-endemic species. Spatial
314 analyses were conducted using the `sf` (Pebesma, 2018; Pebesma & Bivand, 2023), `terra`
315 (Hijmans, 2023), and `exactextractr` (Baston, 2023) packages for vector and raster operations,
316 and visualizations were generated with `ggplot2` (Wickham, 2016).

317 Because ESA-CCI land-cover classes represent structural categories derived from remote
318 sensing rather than vegetation types recognised in major classification schemes, we
319 interpreted both the land-cover associations identified in the NMDS analysis and the spatial
320 patterns of priority woredas in relation to the major vegetation systems described in the Atlas
321 of the Potential Vegetation of Ethiopia (Friis et al., 2010). This approach allowed us to discuss
322 the results within the ecological context of Ethiopia's major vegetations while maintaining
323 consistency with the ESA-CCI land-cover classification used in the analyses

324

325 **3 – RESULTS**

326 ***3.1 – Land-Cover Changes in Ethiopia (1992–2020)***

327 From 1992 to 2020, approximately 6.0% of Ethiopia's land surface (66,651 km²) experienced
328 land-cover change according to the ESA-CCI dataset (Supplementary Figures S2–S4;
329 Supplementary Table S1). The most notable increases were observed in tree-dominated
330 classes, particularly Broadleaf Deciduous Forest, which expanded 14,587 km². Additional
331 increases were recorded in Open Broadleaf Deciduous Forest (+9,264 km²), Mosaic
332 Tree/Shrub >50% (+7,236 km²) and Broadleaf Evergreen Forest (+4,984 km²). Furthermore,
333 Grasslands also showed substantial increase (7,192 km²) during the study period.

334 In contrast, the largest declines occurred in shrub-dominated and mixed vegetation,
335 particularly Shrubland, which experienced the greatest net loss among all ESA classes (-
336 23,451 km²). Substantial reductions were also observed in Mosaic Natural Vegetation (-10,003
337 km²), Bare Areas (-5,377 km²), and Sparse Vegetation (-4,953 km²). Notably, despite their
338 smaller absolute net losses, classes such as Sparse Herbaceous and Needleleaf Evergreen
339 Forest experienced considerable proportional reductions (e.g., >90%), suggesting complete
340 or near-complete conversions at the national scale. Overall, these results indicate that land-
341 cover changes in Ethiopia during the study period were primarily characterised by transitions
342 toward more tree-dominated classes.

343

344 **3.2 – The impact of Range-Mapping Methods on SHI Trends**

345 Our correlation analyses revealed that SHI derived from most geometry-based mapping
346 methods closely matched SDM-based trends (Figure 3; Supplementary Figure S5). Both
347 Pearson (0.714–0.826) and Spearman (0.691–0.798) correlations were high across range
348 mapping methods, indicating a strong agreement in both the direction and relative magnitude
349 of SHI trends. These correlations were statistically significant ($p < 0.05$) for most species:
350 between 90.3% and 93.7% for Pearson, and between 89.3% and 92.2% for Spearman
351 correlations. Among methods, Rapo showed the best overall performance, with the highest
352 average correlation to SDM-based SHI (Pearson = 0.826; Spearman = 0.798) and lowest error
353 (MSE = 341; RMSE = 7.40). The C-hull method also performed well (Pearson = 0.804;
354 Spearman = 0.781; RMSE = 7.30). In contrast, the Buffer (Pearson = 0.714; Spearman =
355 0.691), A-hull (Pearson = 0.760; Spearman = 0.733) and the Country (Pearson = 0.775;
356 Spearman = 0.769) methods performed less effectively, indicating lower capacity to replicate
357 SHI trends derived from SDM.

358 Methods also differed in their ability to produce valid SHI estimates (i.e., those with non-zero
359 area in 1992). Approximately 36.5% (265 species) lacked AOH for at least one range mapping
360 method. However, the number of species lacking suitable AOH—and thus lacking valid SHI
361 estimates—for each range mapping method also varied considerably (Supplementary Figure
362 S6). The Buffer method had the highest number of species without valid SHI (127 species). In
363 contrast, the Country method produced invalid SHI for only three species. C-hull, Rapo, and
364 SDM presented intermediate levels of invalid SHI outputs (18, 23, and 31 species,
365 respectively).

366

367 **3.3 – National SHI for Ethiopia's Flora**

368 Our analysis of the national trends of SHI for Ethiopia's flora showed that median SHI
369 increased by 0.51% between 1992 and 2020, indicating that most Ethiopian species likely
370 experienced modest gains in habitat suitability (Figure 4). Moreover, our linear model showed
371 that both biogeographical status and functional group influenced SHI trends (Table 1;
372 Supplementary Figures S7–S8). Woody, non-endemic species have experienced
373 significantly higher SHI (Estimate = 0.645, SE = 0.065, $p < 0.001$), indicating that this group
374 experienced the most consistent gains in suitable habitat. In contrast, non-woody species had
375 significantly lower SHI slopes relative to woody species (Estimate = -0.388 , SE = 0.089, $p <$
376 0.001), and endemic species also showed significantly lower slopes compared to non-
377 endemics (Estimate = -0.400 , SE = 0.100, $p < 0.001$), suggesting reduced gains or net losses
378 in suitable habitat. Overall, these findings indicate that while some plant groups—particularly

379 woody, non-endemic species—have experienced positive SHI trends, endemic and non-
380 woody species are more likely to be vulnerable to habitat loss.

381

382 **3.4 – Identifying Conservation Priorities through SHI Trends**

383 Our analyses showed that species experiencing declines in their SHI (439 species, of which
384 402 were statistically significant at $p < 0.05$) differed significantly in their associations with
385 ESA-CCI land-cover classes from species exhibiting stable or increasing SHI (574 species,
386 including 535 with statistically significant trends; Figure 5). PERMANOVA showed that these
387 differences explained 17.7% of the variation ($R^2 = 0.177$, $F = 197.5$, $p < 0.001$). NMDS
388 ordination (2D, stress = 0.108) revealed clear separation with only modest overlap between
389 groups (Figure 5A). Land-cover classes like Broadleaf Evergreen Forest (TC-BE, 7.9%),
390 Broadleaf Deciduous Forest (TC-BD, 7.9%), Shrubland (SH, 7.9%), and Deciduous Shrubland
391 (SH-D, 7.8%) emerged as key contributors to overall dissimilarity between groups. Notably,
392 shrub-dominated land-cover classes like Deciduous Shrubland and Shrubland were strongly
393 associated with declining species, while tree-dominated land-cover classes like Broadleaf
394 Deciduous Forest and Broadleaf Evergreen Forest were more closely associated with non-
395 declining species.

396 Spatially, Ethiopia's administrative zones (woredas) of Tselemt (181 species), Beyeda (171),
397 Janamora (170), Meda Welabu (170), and Mena (168) contained the largest numbers of
398 species experiencing declining SHI trends across different species groups (overall, non-
399 endemics, and endemics; Figure 6). For total and non-endemic species, zones with high
400 numbers of declining taxa are more widely distributed, spanning both the central and southern
401 highlands (Fig. 6A-D). In contrast, declining endemic species are more geographically
402 concentrated in the northern highlands of Amhara (Fig. 6E-F), with Janamora (45 endemic
403 species), Beyeda (43), Tselemt (42), Debark (40), and Mena (38) emerging as key hotspots.

404

405 **4 – DISCUSSION**

406 **4.1 – The Impact of Range-Mapping Methods on SHI Trends**

407 We show that geometry-based range mapping methods, especially those producing large
408 spatial extents, yield SHI estimates that closely match those derived from SDMs (Figure 3).
409 This is consistent with earlier evidence suggesting that variation among range map methods
410 has limited impact at broader macroecological patterns (Aronsson et al., 2024). The nature of
411 AOH (and consequently SHI) estimation likely contributes to the observed agreement among

412 methods, as the removal of unsuitable areas mitigates commission errors commonly
413 associated with coarse range maps (Brooks et al., 2019; Lumbierres et al., 2021; Lumbierres
414 et al., 2022). As a result, methods characterised by high commission errors can still perform
415 well in SHI estimation, whereas those prone to high omission errors (e.g., Buffers) tend to
416 exclude suitable habitat, leading to less informative SHI trends.

417 Both correlation and error metrics showed that methods like Rapoport's Mean Proximity
418 polygons (Rapo), and convex hull (C-hull) show the strongest agreement with SDM outputs
419 (Figure 3). Their superior performance relative to broader methods such as Country suggests
420 that some spatial restriction is necessary to reflect historical and ecological limits constraining
421 dispersal. The Rapoport method likely performs well because it adapts to the spatial
422 configuration of occurrence records, generating either broad, continuous ranges (comparable
423 to C-hull and Country) for widely distributed species or smaller, fragmented ranges for
424 restricted species for which records are likely concentrated (Rapoport, 1982; Willis et al., 2003;
425 Rivers et al., 2010). This flexibility enables the method to balance between avoiding omission
426 of suitable habitat while retaining spatial realism for species with a discontinuous distribution,
427 which is particularly relevant in topographically and ecologically complex regions like Ethiopia,
428 where many plant species often have restricted or discontinuous habitat preferences (Friis et
429 al., 2005; Kelbessa & Demissew, 2014).

430 These results underscore the potential applicability of geometry-based methods, particularly
431 Rapo and C-hull, as viable and scalable alternatives for estimating SHI across taxonomic
432 groups or geographic regions for which data are limited. Because these methods require only
433 occurrence data and basic spatial tools (e.g., R packages like *sf* and *rCAT*, Pebesma & Bivand,
434 2023; Moat, 2020), they are particularly useful for hyper-diverse countries in the Global
435 South—e.g., biodiversity hotspots *sensu* Myers et al. (2000)—where governments often face
436 financial and technical capacity constraints in meeting biodiversity monitoring requirements.
437 While lack of comprehensive occurrence data remains a major limitation, these simplified
438 mapping methods offer a way to accelerate biodiversity monitoring by enabling countries to
439 generate species-level habitat indicators rapidly and cost-effectively. This can ultimately
440 improve the pace and scope of biodiversity monitoring, supporting global conservation
441 assessment and planning, as well as reporting capacity against the Global Biodiversity
442 Framework (CBD Secretariat, 2022).

443

444 **4.2 – National SHI for Ethiopia's Flora**

445 At the national scale, median SHI increased slightly (+ 0.51%), suggesting that overall
446 Ethiopian plants have experienced modest gains in habitat area from 1992 to 2020. Woody,

447 non-endemic species show most consistent increase (Estimate = 0.645, SE = 0.065, $p <$
448 0.001; Supplementary Figure S8), suggesting these taxa have likely benefited from land-cover
449 changes. These trends likely reflect the dual advantage of the broad environmental tolerances
450 that characterise species with wide geographic ranges (Jetz et al., 2008), and the enhanced
451 dispersal capacity associated with woody life-forms, especially trees (Beckman & Sullivan,
452 2023), which together facilitate persistence and expansion within changing landscapes. In
453 contrast, the weaker or negative SHI trends observed for endemic species likely reflect their
454 higher sensitivity to habitat change, which has already contributed to documented population
455 declines among many Ethiopian species (Gebrehiwot et al., 2019; Abro et al., 2024). Overall,
456 these findings emphasise that trait-environment interactions—particularly those involving
457 range size and dispersal ability—appear to mediate species' response to land-cover change
458 in Ethiopia, underscoring the need for targeted conservation interventions that account for
459 differences in species' biogeography and function, particularly for endemic and non-woody
460 species at greater risk of habitat loss

461 Nonetheless, the apparently positive scenario for woody, non-endemic species must be
462 interpreted with caution. SHI reflects changes in the extent of structurally suitable habitat but
463 does not capture ecological quality or species-specific viability. The ability of species to
464 colonise newly available habitats depends on several factors, including dispersal capacity, and
465 competition (Zhang et al., 2018), leading to mismatches between potential and realised
466 distributions. In some cases, gains in suitable habitat may reflect anthropogenic reforestation
467 (see Kassa et al., 2022) or afforestation with non-native species (e.g., *Eucalyptus*; Belachew
468 & Minale, 2025), replicating the structural but not functional characteristics of native
469 ecosystems. Similarly, land-cover transitions interpreted as forest expansion may, in fact,
470 represent woody encroachment, a process that is widely documented in Ethiopia (Liao et al.,
471 2018) and that leads to degradation of vegetation quality and reduced capacity to support
472 certain plant species (Rundel et al., 2014). This interpretation is supported by observed shifts
473 from primarily herbaceous (e.g., different types of croplands and savanna; Supplementary
474 Figure S2) to tree-dominated land-cover classes (e.g., Open Broadleaf Deciduous Forest
475 expanded by over 400% in Ethiopia during the study period; Supplementary Figures S3—S4),
476 a pathway that aligns with documented encroachment in Ethiopia (Liao et al., 2018). Thus,
477 SHI trends may overestimate habitat recovery and should ideally be paired with ecological
478 field validation to assess habitat quality.

479

480 **4.3 – Identifying Conservation Priorities through SHI Trends**

481 Our analyses indicate that species experiencing declining SHI trends in Ethiopia are
482 disproportionately associated with shrubland, grassland and mosaic herbaceous ESA-CCI
483 land-cover classes (Figure 5) and are concentrated in woredas (administrative zones) located
484 in northern and southern Ethiopian highlands (Figure 6). Taken together, these findings
485 suggest that species that are increasingly threatened by habitat change are largely
486 concentrated in highland regions where Afro-alpine and Dry Evergreen Afromontane Forest
487 and Grassland Complex vegetation systems occur (Friis et al. 2010). Habitat reduction poses
488 a major threat in these ecosystems, and many constituent species have been documented as
489 experiencing population declines (Gebrehiwot et al., 2019; Abro et al., 2024) due to habitat
490 modification driven by human activities (Nyssen et al., 2014; Tolessa et al., 2017). In particular,
491 the Afro-alpine grasslands—often associated with restricted microenvironmental conditions
492 (Gole et al., 2008)—are increasingly degraded by expanding human settlements and related
493 activities, which have exacerbated habitat degradation and exposed many species to
494 significant threats (Gebrehiwot et al., 2019). As these habitats continue to decline, the survival
495 of many species, especially those with restricted distributions, becomes increasingly
496 threatened, further increasing their extinction risk (Gole et al., 2008; Gebrehiwot et al., 2019;
497 Wang et al. 2020; Abro et al., 2024).

498 Importantly, the Afro-alpine and Dry Evergreen Afromontane Forest and Grassland Complex
499 vegetation systems fall largely outside or only partially overlap with Ethiopia's national
500 protected area network (IUCN ESARO, 2020). This mismatch indicates that Ethiopian plant
501 communities facing the highest pressure from habitat change are also those with the lowest
502 level of formal protection, exacerbating their vulnerability to land-use change and further
503 habitat degradation. The under-protection of these habitats reflects a broader Biome
504 Awareness Disparity (Silveira et al., 2022), where non-tree-dominated vegetation systems
505 such as grasslands, shrublands and savannas receive less attention in conservation policy
506 and funding than forests. Indeed, a recent study by Jago et al. (2025) found that ecosystems
507 like the Ethiopian montane grasslands and woodlands (mostly congruent with Dry Evergreen
508 Afromontane Forest and Grassland Complex in Friis et al. 2010), and the Acacia-Commiphora
509 bushlands and thickets have disproportionately low coverage within the national protected
510 area network. A main concern is that, once degraded, these non-tree-dominated systems
511 rarely recover their original complexity and resilience (Nerlekar & Veldman, 2020; Pilon et al.,
512 2023), making immediate conservation the most effective strategy for mitigating biodiversity
513 loss. In this context, our SHI-based analysis reinforces the urgent need to recognise and
514 protect species in these ecosystems at levels comparable to those of forests (Pilon et al.,
515 2025), not only globally but also within national conservation agendas in Ethiopia.

516 These findings highlight the value of SHI as a tool for identifying conservation priorities beyond
517 traditional biodiversity metrics. By revealing the habitats and zones where plant diversity is
518 declining most severely, SHI provides tools for Ethiopian policymakers and conservation
519 practitioners to target ongoing conservation and restoration efforts to better account for
520 overlooked ecosystems. As Ethiopia advances towards GBF targets, incorporating SHI into
521 its national monitoring framework offers a practical means to better align conservation efforts
522 to ecological priorities. For example, current major conservation and restoration programmes
523 such as Ethiopia's Green Legacy (<https://sdgs.un.org/partnerships/green-legacy-initiative>),
524 the expansion of the protected area network (Langley et al., 2025; Jago et al., 2025), and
525 collaborative identification of Tropical Important Plant Areas (TIPAS; Darbyshire et al., 2017),
526 could benefit from SHI-based assessments to track conservation progress and guide
527 restoration investments.

528

529 ***4.4 – The SHI as an Indicator for the Global Biodiversity Framework***

530 The SHI is a component indicator for the Global Biodiversity Framework (CBD Secretariat,
531 2021; 2022), but its wider application remains constrained by data and processing
532 requirements. Our findings show that relatively simple range-mapping methods can
533 approximate SHI estimations derived from more complex approaches such as SDMs,
534 providing an accessible means for countries to monitor species distributions and address gaps
535 in biodiversity assessments while supporting progress toward international conservation
536 targets. Specifically, the SHI supports Goal A of the GBF (to maintain and restore biodiversity
537 and ecosystem integrity) by tracking suitable habitat for species over time (CBD Secretariat,
538 2021; CBD Secretariat, 2022). Additionally, by allowing the identification of taxa, habitats and
539 geographic regions experiencing most decline, the SHI contributes directly to tracking
540 progress towards Target 2 (restoration of degraded ecosystems) and Target 4 (halting species
541 extinction). As such, the SHI facilitates the national-scale assessment of species' suitable
542 habitats and their trends, which is a key requirement for tracking progress towards biodiversity
543 conservation and ecosystem integrity, thereby providing a robust foundation for evidence-
544 based conservation planning and reporting under the GBF.

545 However, our analyses also highlight several challenges in further refining SHI estimates. For
546 example, while Ethiopia harbours more than 5,500 vascular plant species (Friis et al., 2005;
547 Kelbessa & Demissew, 2014; Demissew et al., 2021), only about 22% (1,247) could be
548 included in our national-scale SHI analysis, largely due to data limitations in the IUCN Red
549 List and occurrence datasets. This coverage gap reflects the low proportion of plant species
550 in global assessments, with approximately 20% assessed on the IUCN Red List compared to

551 near-complete coverage for vertebrates (IUCN, 2024). Moreover, we were unable to generate
552 SHI for some species despite apparently adequate data (i.e., valid range map and complete
553 IUCN textual habitat and elevation information), including cases where AOH was absent for
554 all years analysed (Supplementary Figure S7). While this may partially result from overly
555 restrictive assumptions of our study (e.g., exclusion of marginal habitats), it likely reflects
556 issues with the input data, including poor-quality occurrence records or inaccurate habitat and
557 elevation information for some species.

558 Additionally, although expert-based conversion tables have been shown to perform
559 comparably to data-driven approaches (Lumbierres et al., 2021), effectively linking purely
560 structural land-cover classes to ecologically meaningful habitat types remains a key challenge
561 (Tomaselli et al., 2013; Joppa et al., 2016). While recent efforts (e.g., Jung et al., 2020) have
562 produced spatially explicit habitat classifications aligned with the IUCN habitat classification
563 scheme (IUCN, 2012b), their limited temporal coverage (spanning only 5 years) restricts their
564 utility for long-term SHI assessments. Expanding these datasets to cover broader temporal
565 scales would certainly enhance their applicability in tracking habitat changes and refining SHI
566 estimations.

567 Addressing these limitations is critical to realising SHI as a globally representative and
568 taxonomically inclusive indicator. Key priorities to achieve this are: (i) focusing efforts on
569 mobilising (e.g., through digitisation and georeferencing) and collecting more data; (ii)
570 expanding the Red List assessments for plants and other underrepresented taxa; and (iii)
571 improving the temporal and geographic resolution of land-cover datasets aligned to IUCN
572 habitat schemes. In summary, strengthening these data foundations will be essential to
573 support comprehensive biodiversity monitoring and effective implementation of the Global
574 Biodiversity Framework targets.

575

576 **5 – CONCLUSIONS**

577 This study investigated how different range-mapping approaches influence estimates of the
578 SHI, a biodiversity metric relevant for conservation decisions that may offer a complementary
579 perspective to existing indicators like the Red List Index (RLI; Butchart et al., 2004) and the
580 Living Planet Index (LPI; Ledger et al., 2023). Focusing on plants, a group that is little
581 represented in global biodiversity metrics, we demonstrate that SHI can be feasibly estimated
582 for data-limited taxa and geographic regions using relatively simple approaches. In particular,
583 our findings show that accessible and straightforward mapping approaches can be applied in
584 a hyper-diverse, data-limited context such as Ethiopia, with potential for application in other
585 hyper-diverse countries facing similar data and resources constraints, enabling broader

586 adoption of SHI as a biodiversity monitoring tool. However, continued efforts to improve data
587 collection will be essential for refining SHI estimates and ensuring their reliability for
588 conservation decision-making, ultimately contributing to global efforts to reduce biodiversity
589 loss.

590 At the national scale, we identified uneven declines in suitable habitat across Ethiopia's flora,
591 with endemic and non-woody species associated with non-tree-dominated ecosystems of the
592 highlands experiencing the most severe losses. These declines are especially concerning
593 given that non-tree-dominated ecosystems remain underrepresented in conservation planning
594 (Silveira et al., 2022) and poorly covered by the protected area network in the country,
595 particularly the Afro-alpine, Dry Evergreen Afromontane Forest and Grassland Complex, and
596 the *Acacia–Commiphora* bushlands and thickets (Friis et al., 2010; IUCN ESARO, 2020; Jago
597 et al., 2025). By highlighting both high-risk species groups and priority ecosystems, this study
598 provides an applied framework for monitoring biodiversity trends and informing conservation
599 priorities. As Ethiopia advances implementation of the Global Biodiversity Framework, SHI
600 could serve as a dynamic and objective indicator to support evidence-based conservation
601 planning.

602

603 **6 – DATA AVAILABILITY**

604 Except for data for 203 species, which queued for release in upcoming Red List updates, all
605 data analysed during this study is freely available online without restrictions. The habitat and
606 elevation preferences of species can be accessed on the IUCN Red List
607 (<https://www.iucnredlist.org/>). Occurrence records are available on GBIF
608 (<https://www.gbif.org/>), RAINBIO (<https://gdauby.github.io/rainbio/>) and BIEN
609 (<https://bien.nceas.ucsb.edu/bien/>). Land-cover layers can be found on the European Spatial
610 Agency (<http://maps.elie.ucl.ac.be/CCI/viewer/download.php>). The codes used to perform the
611 analyses in this study are available on GitHub (<https://github.com/moabefferndes/shi-ethiopia>).

613

614 **7 – ACKNOWLEDGMENTS**

615 This research was supported by the Global Centre on Biodiversity for Climate (GCBC) project
616 entitled "*Realising the potential of plant bioresources as nature-based solutions in African*
617 *biodiversity hotspots*."

618

619 **8 – AUTHOR CONTRIBUTION**

620 Moabe F. Fernandes conceived the study, conducted the analyses, and wrote the manuscript.
621 Joseph White contributed to the analyses. James Borrell, Steve Bachman, and Carolina Tovar
622 conceived the study, supervised the research, and contributed to writing and editing. Ermias
623 Lulekal and Sebsebe Demissew provided expert input on Ethiopian vegetation and contributed
624 to manuscript review. Alexandra Roberts, Becca Davis, Emily Terry, Gabriella Hoban, Henry
625 Miller, Seth Ratcliffe, Vida Svahnström, Bezawit Genanaw, Efrata Mekebib, Hanny Lidetu,
626 Lidet Mehari, and Tesfanesh Feseha contributed to data curation and species assessments.
627 Iain Darbyshire and Sileshi Nemomissa contributed to data curation and project
628 administration. Amy Barker and Jack F. Plummer contributed to assessment coordination and
629 project administration. Harry Smith, Jenna Willis, Lynda Murray, Paloma Moore, Andrew
630 Budden, and Liz Brogan contributed to specimen data collation. Tim Pearce and Shambel
631 Alemu contributed to database curation. Kelda F.V.A. Elliott contributed to project coordination.
632 All authors contributed to manuscript review and approved the final version.

633

634 **9 – REFERENCES**

- 635 Abro, T. W., Desta, A. B., Debie, E., & Alemu, D. M. (2024). Endemic plant species and threats
636 to their sustainability in Ethiopia: A systematic review. *Trees, Forests and People*, 17, 100634.
637 <https://doi.org/10.1016/j.tfp.2024.100634>
- 638 Aronsson, H., Zizka, A., Antonelli, A., & Faurby, S. (2024). Expert-based range maps cannot
639 be replicated using data-driven methods but macroecological conclusions arising from them
640 can. *Journal of Biogeography*, 51, 1549–1559. <https://doi.org/10.1111/jbi.14847>
- 641 Asefa, M., Cao, M., He, Y., Mekonnen, E., Song, X., & Yang, J. (2020). Ethiopian vegetation
642 types, climate, and topography. *Plant Diversity*, 42, 302–311.
643 <https://doi.org/10.1016/j.pld.2020.04.004>
- 644 Baston, D. (2023). exactextractr: Fast extraction from raster datasets using polygons. R
645 package version 0.10.0. <https://CRAN.R-project.org/package=exactextractr>
- 646 Beckman, N. G., & Sullivan, L. L. (2023). The causes and consequences of seed dispersal.
647 *Annual Review of Ecology, Evolution, and Systematics*, 54, 403–427.
648 <https://doi.org/10.1146/annurev-ecolsys-102320-104739>
- 649 Belachew, K. G., & Minale, W. K. (2025). Socioeconomic and environmental impacts of
650 Eucalyptus plantations in Ethiopia: An evaluation of benefits, challenges, and sustainable
651 practices. *The Scientific World Journal*, 1780293. <https://doi.org/10.1155/tswj/1780293>

652 Bird, J. P., Buchanan, G. M., Lees, A. C., Clay, R. P., Develey, P. F., Yépez, I., & Butchart, S.
653 H. M. (2012). Integrating spatially explicit habitat projections into extinction risk assessments:
654 A reassessment of Amazonian avifauna incorporating projected deforestation. *Diversity and*
655 *Distributions*, 18, 273–281.

656 Borgelt, J., Sicacha-Parada, J., Skarpaas, O., & Verones, F. (2022). Native range estimates
657 for red-listed vascular plants. *Scientific Data*, 9, 117. [https://doi.org/10.1038/s41597-022-](https://doi.org/10.1038/s41597-022-01233-5)
658 [01233-5](https://doi.org/10.1038/s41597-022-01233-5)

659 Brooks, T. M., Pimm, S. L., Akçakaya, H. R., Buchanan, G. M., Butchart, S. H. M., Foden, W.,
660 Hilton-Taylor, C., Hoffmann, M., Jenkins, C. N., Joppa, L., Li, B. V., Menon, V., Ocampo-
661 Peñuela, N., & Rondinini, C. (2019). Measuring terrestrial area of habitat (AOH) and its utility
662 for the IUCN Red List. *Trends in Ecology & Evolution*, 34, 977–986.
663 <https://doi.org/10.1016/j.tree.2019.06.009>

664 Brown, M. J. M., Walker, B. E., Black, N., Govaerts, R. H. A., Ondo, I., Turner, R., & Nic
665 Lughadha, E. (2023). rWCVP: A companion R package for the World Checklist of Vascular
666 Plants. *New Phytologist*, 240, 1355–1365.

667 Brummitt, R. K. (2001). *World geographic scheme for recording plant distributions* (2nd ed.).
668 Hunt Institute for Botanical Documentation.

669 Butchart, S. H. M., Stattersfield, A. J., Bennun, L. A., Shutes, S. M., Akçakaya, H. R., Baillie,
670 J. E. M., Stuart, S. N., Hilton-Taylor, C., & Mace, G. M. (2004). Measuring global trends in the
671 status of biodiversity: Red List indices for birds. *PLoS Biology*, 2(12), e383.

672 CBD Secretariat. (2021). *Measuring ecosystem integrity (Goal A) in the post-2020 global*
673 *biodiversity framework: The GEO BON species habitat index*.

674 CBD Secretariat. (2022). *Monitoring framework for the Kunming-Montreal Global Biodiversity*
675 *Framework*. Convention on Biological Diversity.

676 Darbyshire, I., Anderson, S., Asatryan, A., Byfield, A., Cheek, M., Clubbe, C., Ghrabi, Z.,
677 Harris, T., Heatubun, C. D., Kalema, J., Magassouba, S., McCarthy, B., Milliken, W., de
678 Montmollin, B., Nic Lughadha, E., Onana, J. M., Saïdou, D., Sârbu, A., Shrestha, K., &
679 Radford, E. A. (2017). Important plant areas: Revised selection criteria for a global approach
680 to plant conservation. *Biodiversity and Conservation*, 26, 1767–1800.
681 <https://doi.org/10.1007/s10531-017-1336-6>

682 Dauby, G., Zaiss, R., Blach-Overgaard, A., Catarino, L., Damen, T., Deblauwe, V., Dessein,
683 S., Dransfield, J., Droissart, V., Duarte, M. C., Engledow, H., Fadeur, G., Figueira, R., Gereau,
684 R. E., Hardy, O. J., Harris, D. J., de Heij, J., Janssens, S., Klomberg, Y., Ley, A. C., Mackinder,

685 B. A., Meerts, P., van de Poel, J. L., Sonké, B., Sosef, M. S. M., Stévant, T., Stoffelen, P.,
686 Svenning, J. C., Sepulchre, P., van der Burgt, X., Wieringa, J. J., & Couvreur, T. L. P. (2016).
687 RAINBIO: A mega-database of tropical African vascular plant distributions. *PhytoKeys*, 74,
688 9723.

689 Demissew, S., Friis, I., & Weber, O. (2021). Diversity and endemism of the flora of Ethiopia
690 and Eritrea: State of knowledge and future perspectives. *Rendiconti Lincei. Scienze Fisiche e*
691 *Naturali*, 32, 675–697.

692 Díaz, S., Settele, J., Brondízio, E. S., Ngo, H. T., Agard, J., Arneeth, A., Balvanera, P., Brauman,
693 K. A., Butchart, S. H. M., Chan, K. M. A., Garibaldi, L. A., Ichii, K., Liu, J., Subramanian, S. M.,
694 Midgley, G. F., Miloslavich, P., Molnár, Z., Obura, D., Pfaff, A., Polasky, S., Purvis, A.,
695 Razzaque, J., Reyers, B., Chowdhury, R. R., Shin, Y. J., Visseren-Hamakers, I., Willis, K. J.,
696 & Zayas, C. N. (2019). Pervasive human-driven decline of life on Earth points to the need for
697 transformative change. *Science*, 366, eaax3100. <https://doi.org/10.1126/science.aax3100>

698 Dinerstein, E., Olson, D., Joshi, A., Vynne, C., Burgess, N. D., Wikramanayake, E., Hahn, N.,
699 Palminteri, S., Hedao, P., Noss, R., Hansen, M., Locke, H., Ellis, E. C., Jones, B., Barber, C.
700 V., Hayes, R., Kormos, C., Martin, V., Crist, E., Sechrest, W., Price, L., Baillie, J. E. M.,
701 Weeden, D., Suckling, K., Davis, C., Sizer, N., Moore, R., Thau, D., Birch, T., Potapov, P.,
702 Turubanova, S., Tyukavina, A., Souza, N., Pinteá, L., Brito, J. C., Llewellyn, O. A., Miller, A.
703 G., Patzelt, A., Ghazanfar, S. A., Timberlake, J., Klöser, H., Shennan-Farpón, Y., Kindt, R.,
704 Lillesø, P. B., van Breugel, P., Graudal, L., Voge, M., Al-Shammari, K. F., & Saleem, M. (2017).
705 An ecoregion-based approach to protecting half the terrestrial realm. *BioScience*, 67, 534–
706 545.

707 Friis, I., Demissew, S., & van Breugel, P. (2010). *Atlas of the Potential Vegetation of Ethiopia*.

708 Friis, I., Thulin, M., Adsersen, H., & Burger, A.-M. (2005). Patterns of plant diversity and
709 endemism in the Horn of Africa. *Biologiske Skrifter*, 55, 289–314.

710 Gebrehiwot, K., Demissew, S., Woldu, Z., Fekadu, M., Desalegn, T., & Teferi, E. (2019).
711 Elevational changes in vascular plants richness, diversity, and distribution pattern in Abune
712 Yosef mountain range, Northern Ethiopia. *Plant Diversity*, 41(4), 220–228.

713 GEO BON. (2015). *Global biodiversity change indicators (Version 1.2)*. Group on Earth
714 Observations Biodiversity Observation Network.

715 Gole, T. W., Borsch, T., Denich, M., & Teketay, D. (2008). Floristic composition and
716 environmental factors characterizing coffee forests in southwest Ethiopia. *Forest Ecology and*
717 *Management*, 255(7), 2138–2150. <https://doi.org/10.1016/j.foreco.2007.12.028>

718 Guisan, A., Thuiller, W., & Zimmermann, N. E. (2017). *Habitat suitability and distribution*
719 *models: With applications in R*. Cambridge University Press.

720 Hamner, B., & Frasco, M. (2018). *Metrics: Evaluation metrics for machine learning*. R package
721 version 0.1.4. <https://CRAN.R-project.org/package=Metrics>

722 Hansen, M. C., Potapov, P. V., Moore, R., Hancher, M., Turubanova, S. A., Tyukavina, A.,
723 Thau, D., Stehman, S. V., Goetz, S. J., Loveland, T. R., Kommareddy, A., Egorov, A., Chini, L.,
724 Justice, C. O., & Townshend, J. R. G. (2013). High-resolution global maps of 21st-century
725 forest cover change. *Science*, 342(6160), 850–853.

726 Hansen, M. C., Stehman, S. V., & Potapov, P. V. (2010). Quantification of global gross forest
727 cover loss. *Proceedings of the National Academy of Sciences*, 107, 8650–8655.

728 Harper, K. L., Lamarche, C., Hartley, A., Peylin, P., Ottlé, C., Bastrikov, V., San Martín, R.,
729 Bohnenstengel, S. I., Kirches, G., Boettcher, M., Shevchuk, R., Brockmann, C., & Defourny,
730 P. (2023). A 29-year time series of annual 300 m resolution plant-functional-type maps for
731 climate models. *Earth System Science Data*, 15, 1465–1499. [https://doi.org/10.5194/essd-15-](https://doi.org/10.5194/essd-15-1465-2023)
732 [1465-2023](https://doi.org/10.5194/essd-15-1465-2023)

733 Hijmans, R. (2023). *terra: Spatial data analysis*. R package version 1.7-65. [https://CRAN.R-](https://CRAN.R-project.org/package=terra)
734 [project.org/package=terra](https://CRAN.R-project.org/package=terra)

735 Hijmans, R. J., Barbosa, M., Ghosh, A., & Mandel, A. (2023). *geodata: Download geographic*
736 *data*. R package version 0.5-9. <https://CRAN.R-project.org/package=geodata>

737 IUCN. (2012a). *IUCN Red List categories and criteria: Version 3.1*. IUCN.

738 IUCN. (2012b). *Habitats classification scheme (version 3.1)*.
739 <https://www.iucnredlist.org/resources/habitat-classification-scheme>

740 IUCN. (2016). *A global standard for the identification of key biodiversity areas*.

741 IUCN. (2024). *The IUCN Red List of threatened species*. <https://www.iucnredlist.org> Accessed
742 on 24 July 2024

743 IUCN ESARO. (2020) *State of Protected and Conserved Areas Report Series No. 1*. IUCN
744 ESARO.

745 Jago, S., Gizaw, G., Genanaw, B., Langley, J., Lulekal, E., White, J. D. M., Rowlands, A. N.,
746 Geda, T., Wakjira, K., Regassa, F., Demissew, S., Woldeyes, F., Abebe, W., Jones, J. P. G.,
747 Smith, R. J., & Borrell, J. (2025). Trade-offs between nature and people reveal challenges in
748 translating global conservation targets into national realities. *EcoEvoRxiv*.
749 <https://doi.org/10.32942/X2306T>

750 Jetz, W., Şekercioğlu, Ç. H., & Watson, J. E. M. (2008). Ecological correlates and conservation
751 implications of overestimating species geographic ranges. *Conservation Biology*, 22(1), 110–
752 119. <https://doi.org/10.1111/j.1523-1739.2007.00847.x>

753 Jetz, W., McGeoch, M. A., Guralnick, R., Ferrier, S., Beck, J., Costello, M. J., Fernandez, M.,
754 Geller, G. N., Keil, P., Merow, C., Meyer, C., Muller-Karger, F. E., Pereira, H. M., Regan, E. C.,
755 Schmeller, D. S., & Turak, E. (2019). Essential biodiversity variables for mapping and
756 monitoring species populations. *Nature Ecology & Evolution*, 3, 539–551.
757 <https://doi.org/10.1038/s41559-019-0826-1>

758 Jetz, W., McGowan, J., Rinnan, D. S., Possingham, H. P., Visconti, P., O'Donnell, B., &
759 Londoño-Murcia, M. C. (2022). Include biodiversity representation indicators in area-based
760 conservation targets. *Nature Ecology & Evolution*, 6, 123–126.
761 <https://doi.org/10.1038/s41559-021-01620-y>

762 Jetz, W., McPherson, J. M., & Guralnick, R. P. (2012). Integrating biodiversity distribution
763 knowledge: Toward a global map of life. *Trends in Ecology & Evolution*, 27, 151–159.
764 <https://doi.org/10.1016/j.tree.2011.09.007>

765 Joppa, L. N., O'Connor, B., Visconti, P., Smith, C., Geldmann, J., Hoffmann, M., Watson, J. E.
766 M., Butchart, S. H. M., Virah-Sawmy, M., Halpern, B. S., Ahmed, S. E., Balmford, A.,
767 Sutherland, W. J., Harfoot, M., Hilton-Taylor, C., Foden, W., Di Minin, E., Pagad, S., Genovesi,
768 P., Hutton, J., & Burgess, N. D. (2016). Filling in biodiversity threat gaps. *Science*, 352, 199.

769 Jung, M., Dahal, P. R., Butchart, S. H. M., Donald, P. F., De Lamo, X., Lesiv, M., Kapos, V.,
770 Rondinini, C., & Visconti, P. (2020). A global map of terrestrial habitat types. *Scientific Data*, 7,
771 256. <https://doi.org/10.1038/s41597-020-00599-8>

772 Kassa, H., Abiyu, A., Hagazi, N., Mokria, M., Kassawmar, T., & Gitz, V. (2022). Forest
773 landscape restoration in Ethiopia: Progress and challenges. *Frontiers in Forests and Global
774 Change*, 5, 796106. <https://doi.org/10.3389/ffgc.2022.796106>

775 KBA Standards and Appeals Committee. (2019). *Guidelines for using a global standard for the
776 identification of key biodiversity areas*. IUCN

777 Kelbessa, E., & Demissew, S. (2014). Diversity of vascular plant taxa of the flora of Ethiopia
778 and Eritrea. *Ethiopian Journal of Biological Sciences*, 13, 37–45.

779 Langley, J., Starnes, T., Fernandes, M., Bachman, S., Plumtre, A. J., Crowe, O., Kor, L., Jago,
780 S., Perez, F., Smith, R. J., White, J. D. M., Tovar, C., Darbyshire, I., & Borrell, J. (2025). Key
781 biodiversity areas and important plant areas can help build ecologically representative

782 protected and conserved area networks to meet 30-by-30. *EcoEvoRxiv*.
783 <https://doi.org/10.32942/X27S7C>

784 Ledger, S. E. H., Loh, J., Almond, R., Böhm, M., Clements, C. F., Currie, J., Deinet, S.,
785 Galewski, T., Grooten, M., Jenkins, M., Marconi, V., Painter, B., Scott-Gatty, K., Young, L.,
786 Hoffmann, M., Freeman, R., & McRae, L. (2023). Past, present, and future of the Living Planet
787 Index. *npj Biodiversity*, 2, 12. <https://doi.org/10.1038/s44185-023-00017-3>

788 Liao, C., Clark, P. E., & DeGloria, S. D. (2018). Bush encroachment dynamics and rangeland
789 management implications in southern Ethiopia. *Ecology and Evolution*, 8, 11694–11703.
790 <https://doi.org/10.1002/ece3.4621>

791 Lumbierres, M., Dahal, P. R., Di Marco, M., Butchart, S. H. M., Donald, P. F., & Rondinini, C.
792 (2021). Translating habitat class to land cover to map area of habitat of terrestrial vertebrates.
793 *Conservation Biology*, 36, e13851. <https://doi.org/10.1111/cobi.13851>

794 Lumbierres, M., Dahal, P. R., Soria, C. D., Di Marco, M., Butchart, S. H. M., Donald, P. F., &
795 Rondinini, C. (2022). Area of habitat maps for the world's terrestrial birds and mammals.
796 *Scientific Data*, 9, 749. <https://doi.org/10.1038/s41597-022-01838-w>

797 Mittermeier, R. A., Gil, P. R., Hoffmann, M., Pilgrim, J., Brooks, T., Mittermeier, C. G.,
798 Lamoreux, J., & Fonseca, G. A. B. (2005). *Hotspots revisited: Earth's biologically richest and*
799 *most endangered terrestrial ecoregions*. Conservation International.

800 Moat, J. (2020). *rCAT: Conservation assessment tools*. R package.

801 Myers, N., Mittermeier, R. A., Mittermeier, C. G., Fonseca, G. A. B., & Kent, J. (2000).
802 Biodiversity hotspots for conservation priorities. *Nature*, 403, 853–858.

803 Nerlekar, A. N., & Veldman, J. W. (2020). High plant diversity and slow assembly of old-growth
804 grasslands. *Proceedings of the National Academy of Sciences*, 117, 18550–18556.
805 <https://doi.org/10.1073/pnas.1922266117>

806 Nyssen, J., Frankl, A., Haile, M., Hurni, H., Descheemaeker, K., Crummey, D., Ritler, A.,
807 Portner, B., Nievergelt, B., Moeyersons, J., Munro, N., Deckers, J., Billi, P., & Poesen, J.
808 (2014). Environmental conditions and human drivers for changes to north Ethiopian mountain
809 landscapes over 145 years. *Science of the Total Environment*, 485, 164–179.

810 Oksanen, J., Simpson, G., Blanchet, F., Kindt, R., Legendre, P., Minchin, P., O'Hara, R.,
811 Solymos, P., Stevens, M., Szoecs, E., Wagner, H., Barbour, M., Bedward, M., Bolker, B.,
812 Borcard, D., Borman, T., Carvalho, G., Chirico, M., De Cáceres, M., Durand, S., Evangelista,
813 H., FitzJohn, R., Friendly, M., Furneaux, B., Hannigan, G., Hill, M., Lahti, L., Martino, C.,

814 McGlinn, D., Ouellette, M., Ribeiro Cunha, E., Smith, T., Stier, A., Ter Braak, C., & Weedon, J.
815 (2025). *vegan: Community ecology package*. R package.

816 Pebesma, E. (2018). *Simple features for R: Standardized support for spatial vector data*. *The*
817 *R Journal*, 10(1), 439–446.

818 Pebesma, E., & Bivand, R. (2023). *Spatial data science: With applications in R*. Chapman and
819 Hall/CRC.

820 Pettorelli, N., Safi, K., & Turner, W. (2014). Introduction: Satellite remote sensing, biodiversity
821 research, and conservation of the future. *Philosophical Transactions of the Royal Society B*,
822 369, 20130190.

823 Phillips, S. J., Anderson, R. P., & Schapire, R. E. (2006). Maximum entropy modeling of
824 species geographic distributions. *Ecological Modelling*, 190, 231–259.
825 <https://doi.org/10.1016/j.ecolmodel.2005.03.026>

826 Pilon, N., Campos, B. H., Durigan, G., Cava, M. G., Rowland, L., Schmidt, I., Sampaio, A., &
827 Oliveira, R. S. (2023). Challenges and directions for open ecosystems biodiversity restoration.
828 *Journal of Applied Ecology*, 60, 849–858. <https://doi.org/10.1111/1365-2664.14368>

829 Pilon, N., Peixoto, F., Oliveira, R. S., Oliveira, A. C. A., et al. (2025). Open letter: There are
830 more than just trees and forests to be conserved and restored. *Plants, People, Planet*,
831 10.1002/ppp3.10635

832 Powers, R. P., & Jetz, W. (2019). Global habitat loss and extinction risk of terrestrial
833 vertebrates under future land-use-change scenarios. *Nature Climate Change*, 9, 323–329.

834 Rapoport, E. H. (1982). *Areography: Geographical strategies of species*. Pergamon Press.

835 R Core Team. (2025). *R: A language and environment for statistical computing*. R Foundation
836 for Statistical Computing.

837 Ribeiro, B. R., Velazco, S. J., Guidoni-Martins, K., Tessarolo, G., Jardim, L., Bachman, S. P.,
838 & Loyola, R. (2022). bdc: A toolkit for standardizing, integrating, and cleaning biodiversity data.
839 *Methods in Ecology and Evolution*, 13, 1421–1428. <https://doi.org/10.1111/2041-210X.13868>

840 Rivers, M. C., Bachman, S. P., Meagher, T. R., Nic Lughadha, E., & Brummitt, N. A. (2010).
841 Subpopulations, locations, and fragmentation: Applying IUCN Red List criteria to herbarium
842 specimen data. *Biodiversity and Conservation*, 19, 2071–2085.
843 <https://doi.org/10.1007/s10531-010-9826-9>

844 Rondinini, C., Di Marco, M., Chiozza, F., Santulli, G., Baisero, D., Visconti, P., Hoffmann, M.,
845 Schipper, J., Stuart, S. N., Tognelli, M. F., Amori, G., Falcucci, A., Maiorano, L., & Boitani, L.

846 (2011). Global habitat suitability models of terrestrial mammals. *Philosophical Transactions of*
847 *the Royal Society B*, 366, 2633–2641.

848 Rondinini, C., Wilson, K. A., Boitani, L., Grantham, H., & Possingham, H. P. (2006). Tradeoffs
849 of different types of species occurrence data for use in systematic conservation planning.
850 *Ecology Letters*, 9, 1136–1145.

851 Rundel, P. W., Dickie, I. A., & Richardson, D. M. (2014). Tree invasions into treeless areas:
852 Mechanisms and ecosystem processes. *Biological Invasions*, 16, 663–675.

853 Runfola, D., Anderson, A., Baier, H., Crittenden, M., Dowker, E., Fuhrig, S., Goodman, S.,
854 Grimsley, G., Layko, R., Melville, G., Mulder, M., Oberman, R., Panganiban, J., Peck, A., Seitz,
855 L., Shea, S., Slevin, H., Youngerman, R., & Hobbs, L. (2020). geoBoundaries: A global
856 database of political administrative boundaries. *PLoS ONE*, 15(4), e0231866.

857 Santini, L., Butchart, S. H. M., Rondinini, C., Benítez-López, A., Hilbers, J. P., Schipper, A. M.,
858 Cengic, M., Tobias, J. A., & Huijbregts, M. A. J. (2019). Applying habitat and population-density
859 models to land-cover time series to inform IUCN Red List assessments. *Conservation Biology*,
860 33, 1084–1093.

861 Silveira, F. A. O., Ordóñez-Parra, C. A., Moura, L. C., Schmidt, I. B., Andersen, A. N., Bond,
862 W., Buisson, E., Durigan, G., Fidelis, A., Oliveira, R. S., Parr, C., Rowland, L., Veldman, J. W.,
863 & Pennington, R. T. (2022). Biome awareness disparity is BAD for tropical ecosystem
864 conservation and restoration. *Journal of Applied Ecology*, 59, 1967–1975.

865 Simkin, R. D., Seto, K. C., McDonald, R. I., & Jetz, W. (2022). Biodiversity impacts and
866 conservation implications of urban land expansion projected to 2050. *Proceedings of the*
867 *National Academy of Sciences*, 119, e2117297119.

868 Tittensor, D. P., Walpole, M., Hill, S. L. L., Boyce, D. G., et al. (2014). A mid-term analysis of
869 progress toward international biodiversity targets. *Science*, 346, 241–244.

870 Tolessa, T., Senbete, F., & Kidane, M. (2017). The impact of land use/land cover change on
871 ecosystem services in the central highlands of Ethiopia. *Ecosystem Services*, 23, 47–54.

872 Tomaselli, V., Dimopoulos, P., Marangi, C., Kallimanis, A. S., Adamo, M., Tarantino, C.,
873 Panitsa, M., Terzi, M., Veronico, G., Lovergine, F., Nagendra, H., Lucas, R., Mairota, P.,
874 Múcher, C. A., & Blonda, P. (2013). Translating land cover classifications to habitat taxonomies
875 for landscape monitoring. *Landscape Ecology*, 28, 905–930.

876 van Proosdij, A. S. J., Sosef, M. S. M., Wieringa, J. J., & Raes, N. (2016). Minimum required
877 number of specimen records to develop accurate species distribution models. *Ecography*, 39,
878 542–552.

879 Velazco, S. J., Rose, M. B., de Andrade, A. F., Minoli, I., & Franklin, J. (2022). flexsdm: An R
880 package for supporting a comprehensive and flexible species distribution modelling workflow.
881 *Methods in Ecology and Evolution*, 13, 1661–1669.

882 Vignali, S., Barras, A. G., Arlettaz, R., & Braunisch, V. (2020). SDMtune: An R package to tune
883 and evaluate species distribution models. *Ecology and Evolution*, 10, 11488–11506.

884 Visconti, P., Bakkenes, M., Baisero, D., Brooks, T., Butchart, S. H. M., Joppa, L., Alkemade,
885 R., Di Marco, M., Santini, L., Hoffmann, M., Maiorano, L., Pressey, R. L., Arponen, A., Boitani,
886 L., Reside, A. E., van Vuuren, D. P., & Rondinini, C. (2016). Projecting global biodiversity
887 indicators under future development scenarios. *Conservation Letters*, 9, 5–13.

888 Wang, S. W., Boru, B. H., Njogu, A. W., Ochola, A. C., Hu, G. W., Zhou, Y. D., & Wang, Q. F.
889 (2020). Floristic composition and endemism pattern of vascular plants in Ethiopia and Eritrea.
890 *Journal of Systematics and Evolution*, 58, 33–42.

891 Wickham, H., François, R., Henry, L., Müller, K., & Vaughan, D. (2023). *dplyr: A grammar of*
892 *data manipulation*. R package.

893 Wickham, H. (2016). *ggplot2: Elegant graphics for data analysis*. Springer.

894 Willis, F., Moat, J., & Paton, A. (2003). Defining a role for herbarium data in Red List
895 assessments: A case study of *Plectranthus* from eastern and southern tropical Africa.
896 *Biodiversity and Conservation*, 12, 1537–1552.

897 Zhang, H., Qi, W., & Liu, K. (2018). Functional traits associated with plant colonizing and
898 competitive ability influence species abundance during secondary succession. *Ecology and*
899 *Evolution*, 8, 6529–6536.

900 Zizka, A., Silvestro, D., Andermann, T., Azevedo, J., Ritter, C. D., Edler, D., Farooq, H.,
901 Herdean, A., Ariza, M., Scharn, R., Svantesson, S., Wengström, N., Zizka, V., & Antonelli, A.
902 (2019). CoordinateCleaner: Standardized cleaning of occurrence records from biological
903 collection databases. *Methods in Ecology and Evolution*, 10, 744–751.

904

905

906 **TABLES AND FIGURES**

907 Table 1. Parameter estimates from the linear model examining the effects of biogeographical status and functional
 908 group on SHI trends.

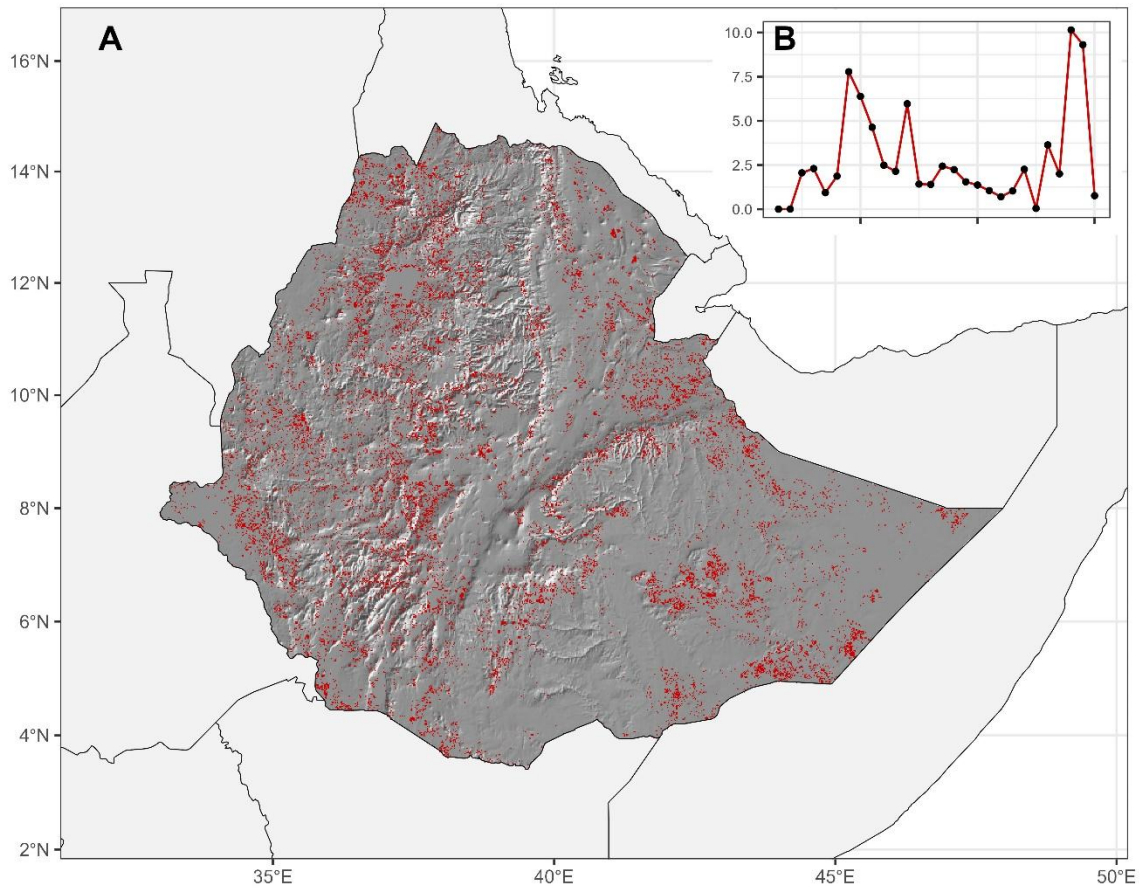
Linear Model Predicting SHI Slope					
Effect of Life Form and Endemism					
Predictor	Estimate	Std. Error	95% CI (Lower)	95% CI (Upper)	p-value
Woody, Non-endemic (Intercept)	0.645	0.065	0.518	0.773	< 0.001
Non-woody (vs. Woody)	-0.388	0.089	-0.562	-0.213	< 0.001
Endemic (vs. Non-endemic)	-0.400	0.100	-0.596	-0.204	< 0.001
Model: <code>lm(slope ~ life_form + endemcity)</code>					

909

910 SHI trends are represented by slope coefficients derived from species-specific regressions over time.

911

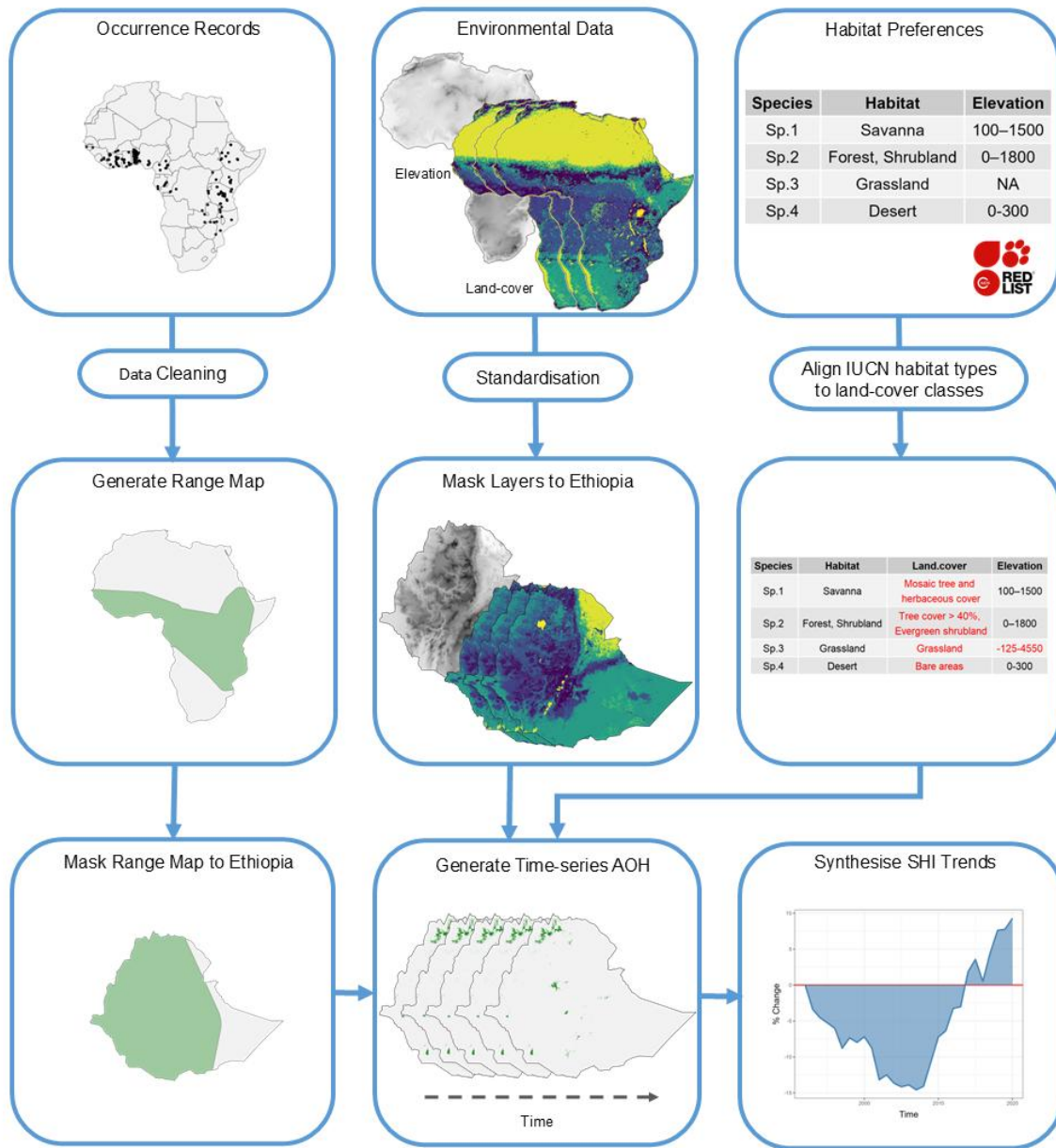
912



913

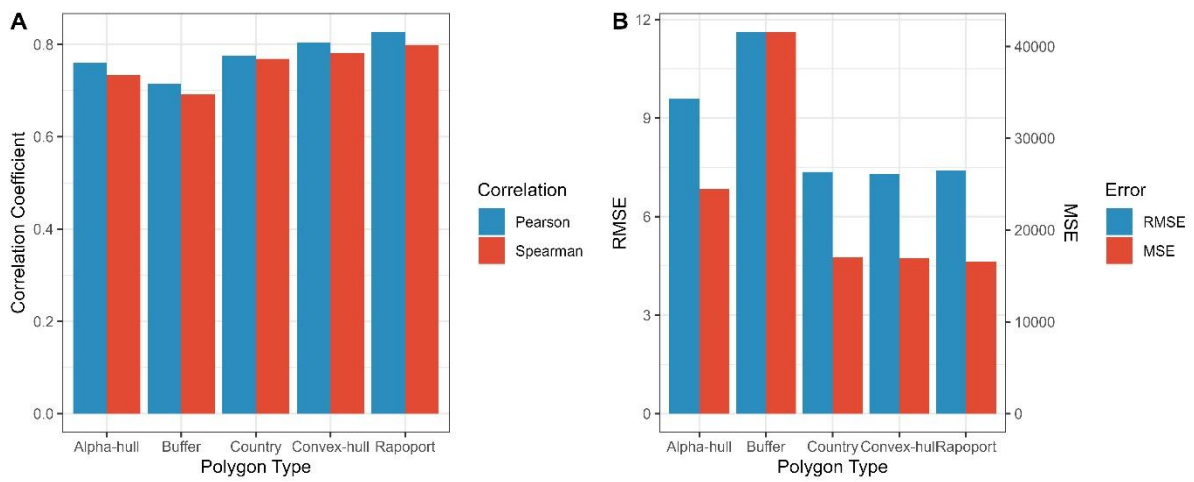
914 Figure 1. Spatial distribution and temporal trends of land-cover modification in Ethiopia from 1992 to 2020. (A) Map
915 showing the spatial extent of land-cover modification, with red cells indicating areas of change overlaid over
916 topographic hillshade. (B) Annual total area of land-cover modification (thousands of km²) over time. Overall,
917 approximately 6% of Ethiopia's total area has experienced land-cover modification between 1992 and 2020, with
918 peaks between 1998–2000 and 2017–2019. Both graphics are based on the assessment of 25 land-cover classes
919 as depicted in products developed by the European Space Agency (ESA; Harper et al., 2023).

920



923 Figure 2. Analytical workflow for estimating SHI from species occurrences, habitat, and land-cover data.
 924 Occurrence records are processed to generate range maps for individual species, which are masked to the area
 925 of interest. Elevation and land-cover layers are rescaled and masked accordingly to ensure compatibility of further
 926 geospatial operations. Additionally, an expert-based conversion table (e.g., available in Santini *et al.*, 2019) is
 927 employed to align IUCN habitat preferences information with the European Space Agency (ESA) land-cover
 928 classes (Harper *et al.*, 2023). In the analyses, the intersection of species ranges with suitable habitat and elevation
 929 layers produces annual Area of Habitat (AOH) maps from 1992 to 2020. This time-series AOH is used to calculate
 930 the SHI as the percent change in suitable habitat over time relative to 1992. This final SHI for multiple species can
 931 be aggregated into a regional or country-level index.

933



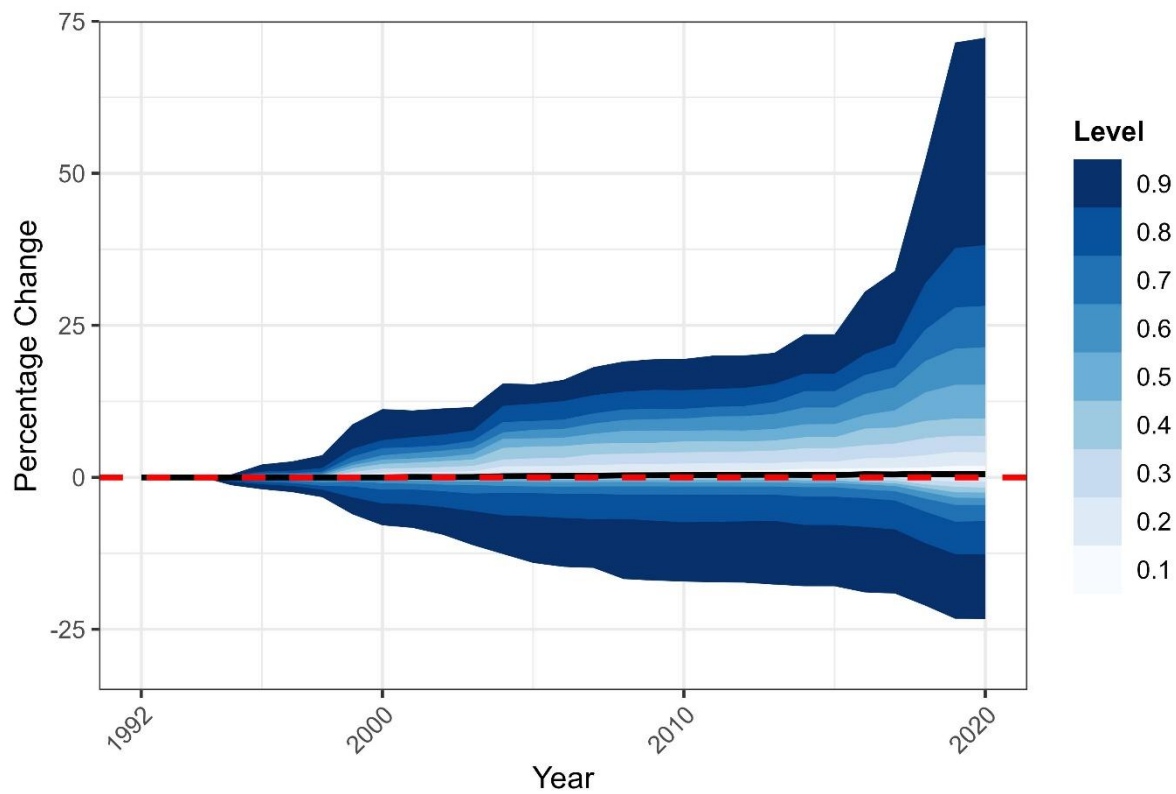
934

935 Figure 3. Agreement between SHI estimates derived from SDMs and alternative geometry-based range-mapping
936 methods. (A) Pearson and Spearman correlation coefficients. (B) Root Mean Squared Error (RMSE) and Mean
937 Squared Error (MSE). All geometry-based methods show significant correlations with SDM-based SHI; MSE values
938 are rescaled for visualisation while maintaining the correct relative differences.

939

940

941

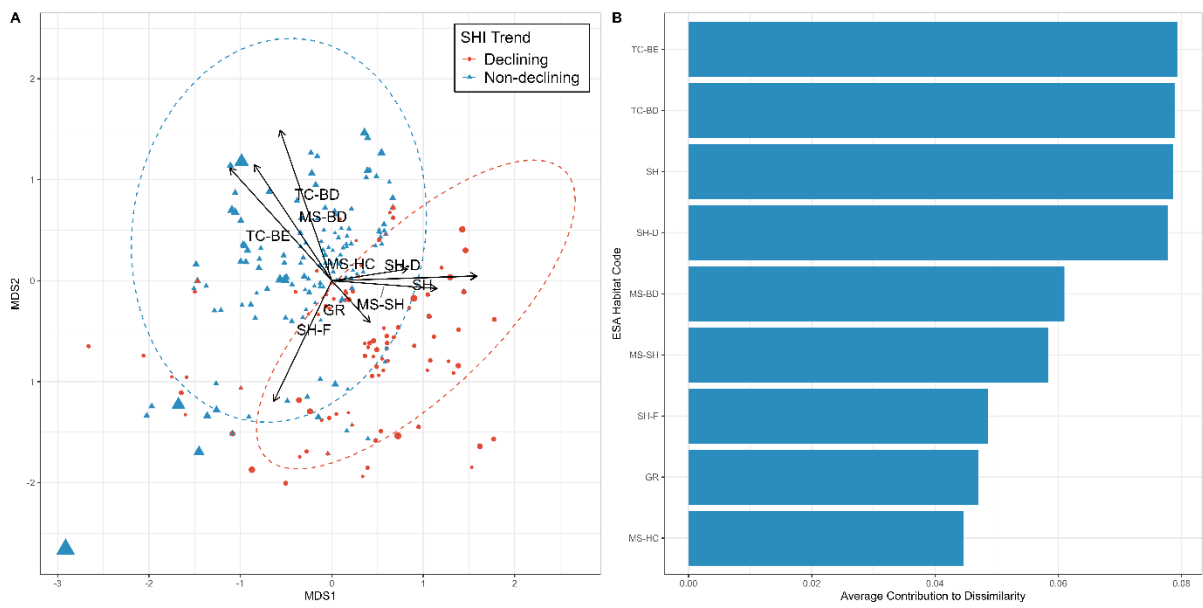


942

943 Figure 4. Summary of SHI changes for Ethiopian plant species from 1992 to 2020. Line ribbon charts show changes
944 in percentage of area (measured as the number of 1 x 1km cells), with coloured bands representing the proportion
945 of species within a particular 10%-interval class. The black line indicates the median SHI change across species.

946

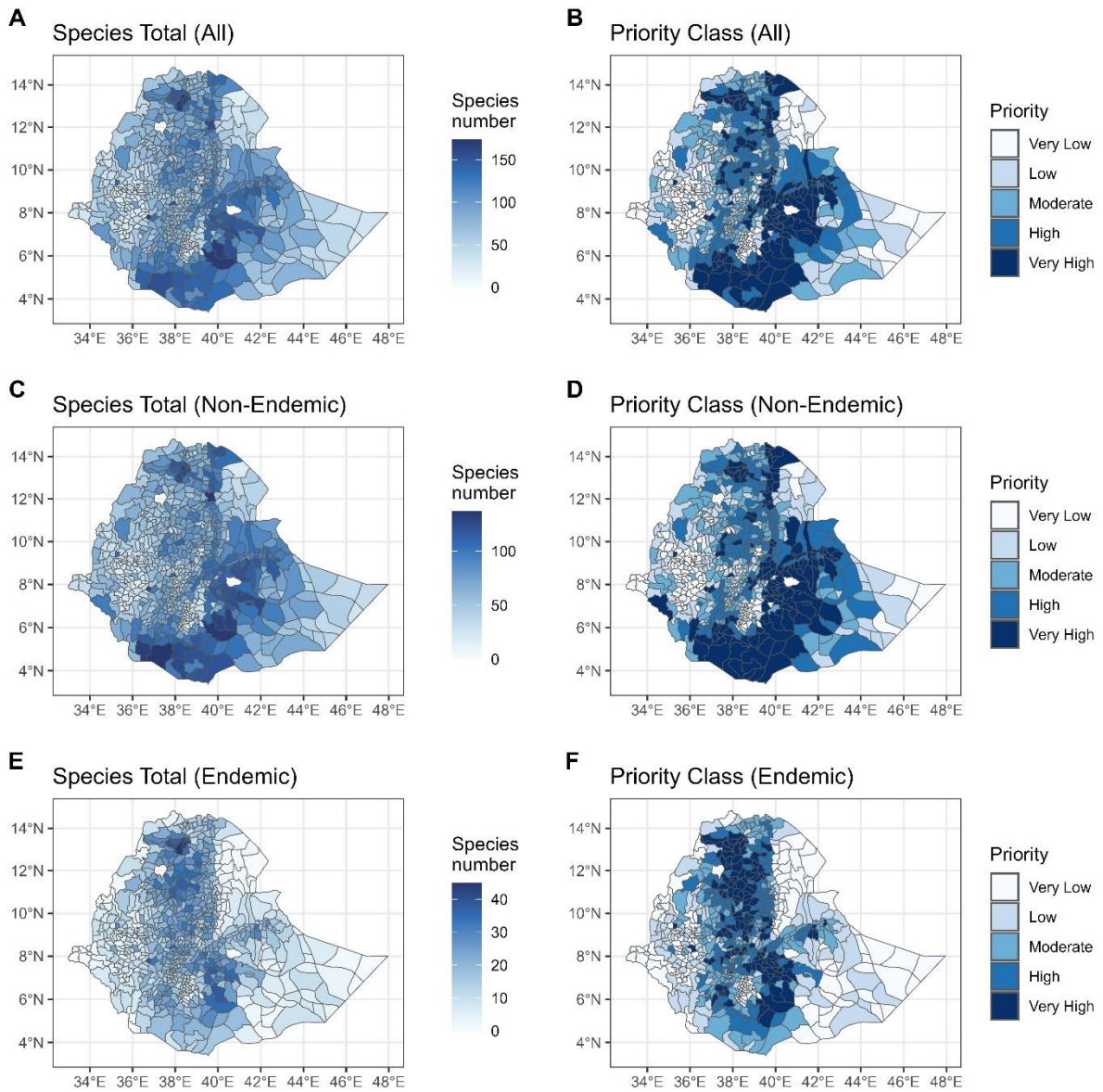
947



948

949 Figure 5. Differences in ESA-CCI land-cover class associations between declining and non-declining species. (A)
950 NMDS ordination of species' land-cover associations (Jaccard dissimilarities), with symbols and colours indicating
951 SHI trend class and size proportional to the absolute value of SHI slope (*i.e.*, the magnitude of change). Dashed
952 ellipses indicate 95% confidence regions for each group. Overlaid vectors represent ESA land-cover classes
953 contributing strongly to group separation, as identified by SIMPER analysis. (B) Relative contribution of the top
954 ESA land-cover classes to dissimilarity between groups (SIMPER analysis). Land-cover classes are ordered by
955 contribution and labelled using ESA codes (GR: Grassland; SH: Shrubland; SH-D: Deciduous shrubland; SH-F:
956 Shrub/herbaceous, flooded; MS-BD: Mosaic tree, shrub; MS-HC: Mosaic herbaceous >50%; MS-SH: Mosaic shrub
957 >50%; TC-BE: Tree cover, broadleaf evergreen; TC-DB: Tree cover, broadleaf deciduous).

958



959

960 Figure 6. Spatial distribution of species with declining SHI and corresponding conservation priority zones (woredas)
 961 in Ethiopia. (A–C) Number of species with declining habitat per zone. (D–F) Priority classes based on quintile ranks
 962 of declining species in each zone, ranging from Very Low to Very High. Panels show results for all species (A, D),
 963 non-endemic species only (B, E), and endemic species only (C, F).

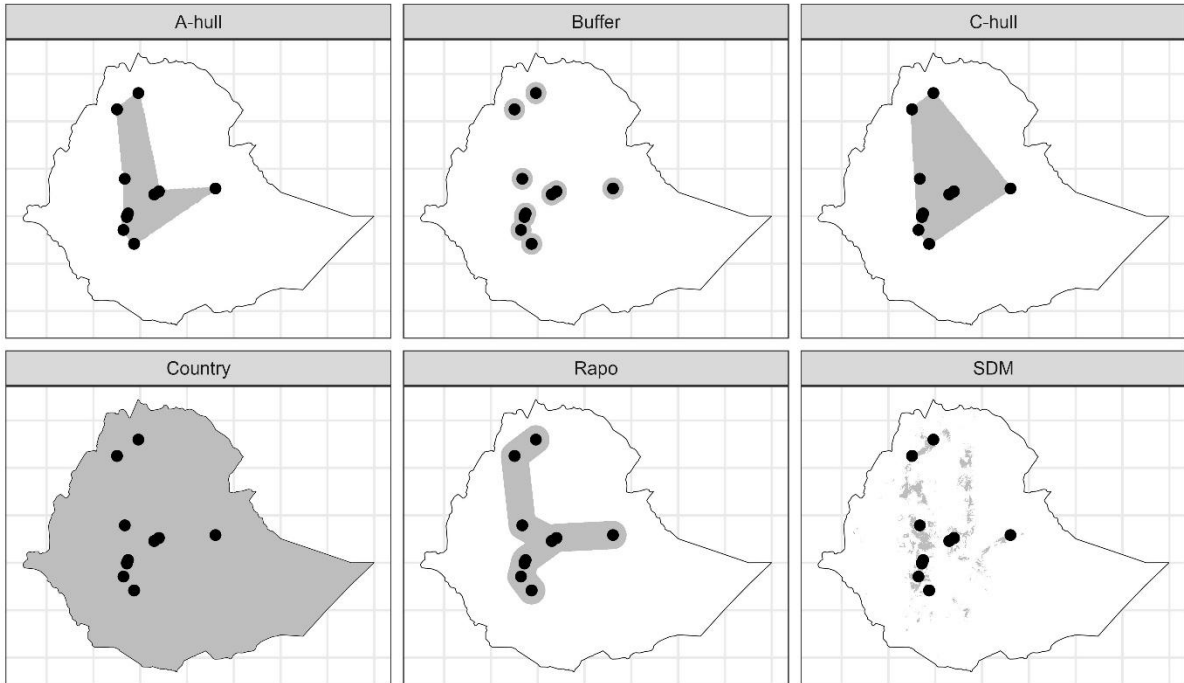
964

965

966 **SUPPLEMENTARY MATERIAL**967 **SUPPLEMENTARY TABLES AND FIGURES**

968 Table S1. Summary of land-cover change by ESA-CCI class in Ethiopia (1992–2020)

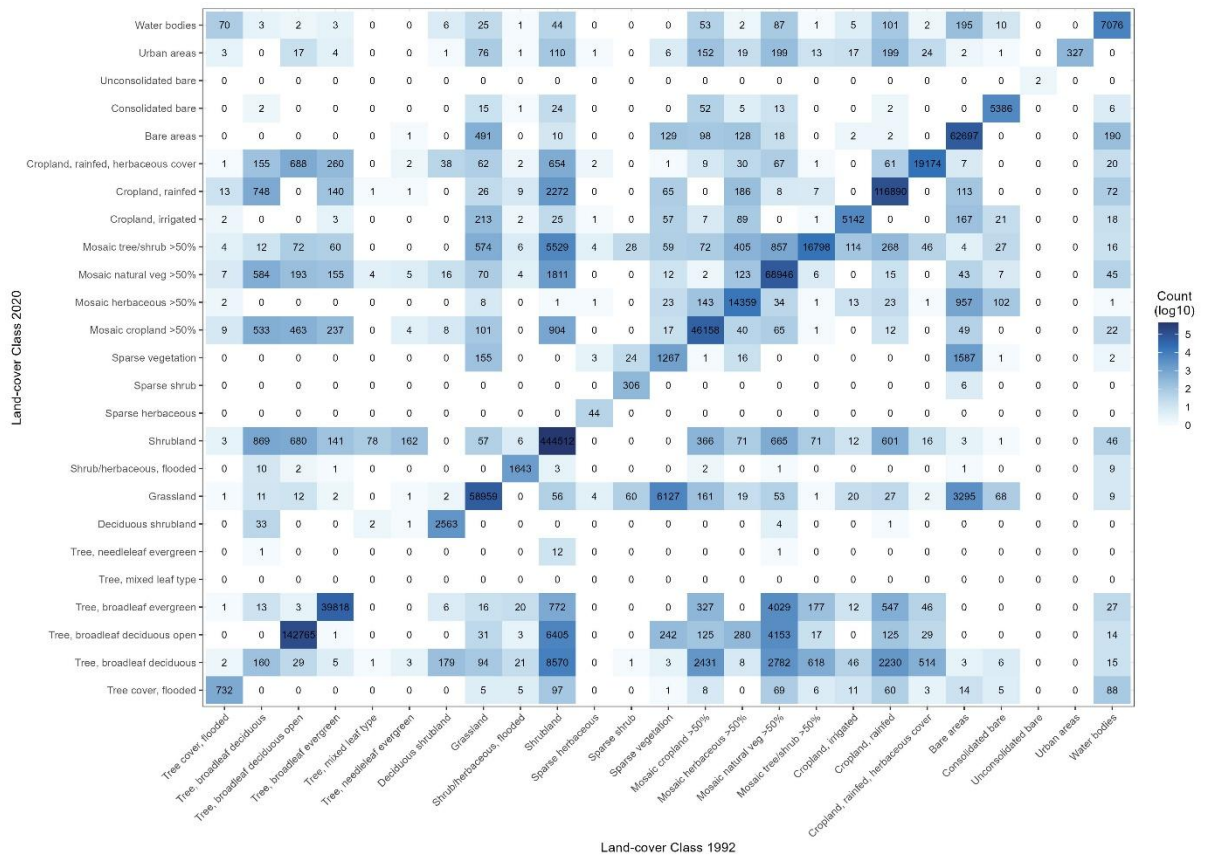
Land-Cover Class	Land-Cover Change (ESA Classes)				
	Change (1992-2020)			Relative Metrics	
	Gain (km ²)	Loss (km ²)	Net Change (km ²)	Class-Level Change (%)	Share of Total Change (%)
Tree cover, flooded	372	118	254	29.88	0.27
Tree, broadleaf deciduous	17,561	2,974	14,587	465.44	15.58
Tree, broadleaf deciduous open	11,425	2,161	9,264	6.39	9.89
Tree, broadleaf evergreen	5,996	1,012	4,984	12.21	5.32
Tree, mixed leaf type	0	86	-86	-100.00	0.09
Tree, needleleaf evergreen	14	180	-166	-92.22	0.18
Deciduous shrubland	41	256	-215	-7.63	0.23
Grassland	9,931	2,019	7,912	12.98	8.45
Shrub/herbaceous, flooded	29	81	-52	-3.02	0.06
Shrubland	3,848	27,299	-23,451	-4.97	25.04
Sparse herbaceous	0	16	-16	-26.67	0.02
Sparse shrub	6	113	-107	-25.54	0.11
Sparse vegetation	1,789	6,742	-4,953	-61.84	5.29
Mosaic cropland >50%	2,465	4,009	-1,544	-3.08	1.65
Mosaic herbaceous >50%	1,310	1,421	-111	-0.70	0.12
Mosaic natural veg >50%	3,102	13,105	-10,003	-12.19	10.68
Mosaic tree/shrub >50%	8,157	921	7,236	40.84	7.73
Cropland, irrigated	606	252	354	6.56	0.38
Cropland, rainfed	3,661	4,274	-613	-0.51	0.65
Cropland, rainfed, herbaceous cover	2,060	683	1,377	6.93	1.47
Bare areas	1,069	6,446	-5,377	-7.78	5.74
Consolidated bare	120	249	-129	-2.29	0.14
Unconsolidated bare	0	0	0	0.00	0.00
Urban areas	845	0	845	258.41	0.90
Water bodies	610	600	10	0.13	0.01



970

971 Figure S1. Examples of geometry-based range mapping methods used to estimate SHI for plant species in
 972 Ethiopia. Each panel shows a different method applied to the same set of occurrence records (black dots). The
 973 shaded polygons represent the inferred range map using alpha hull, buffer, convex hull, country-wide extent,
 974 Rapoport's mean propinquity method and SDM approaches.

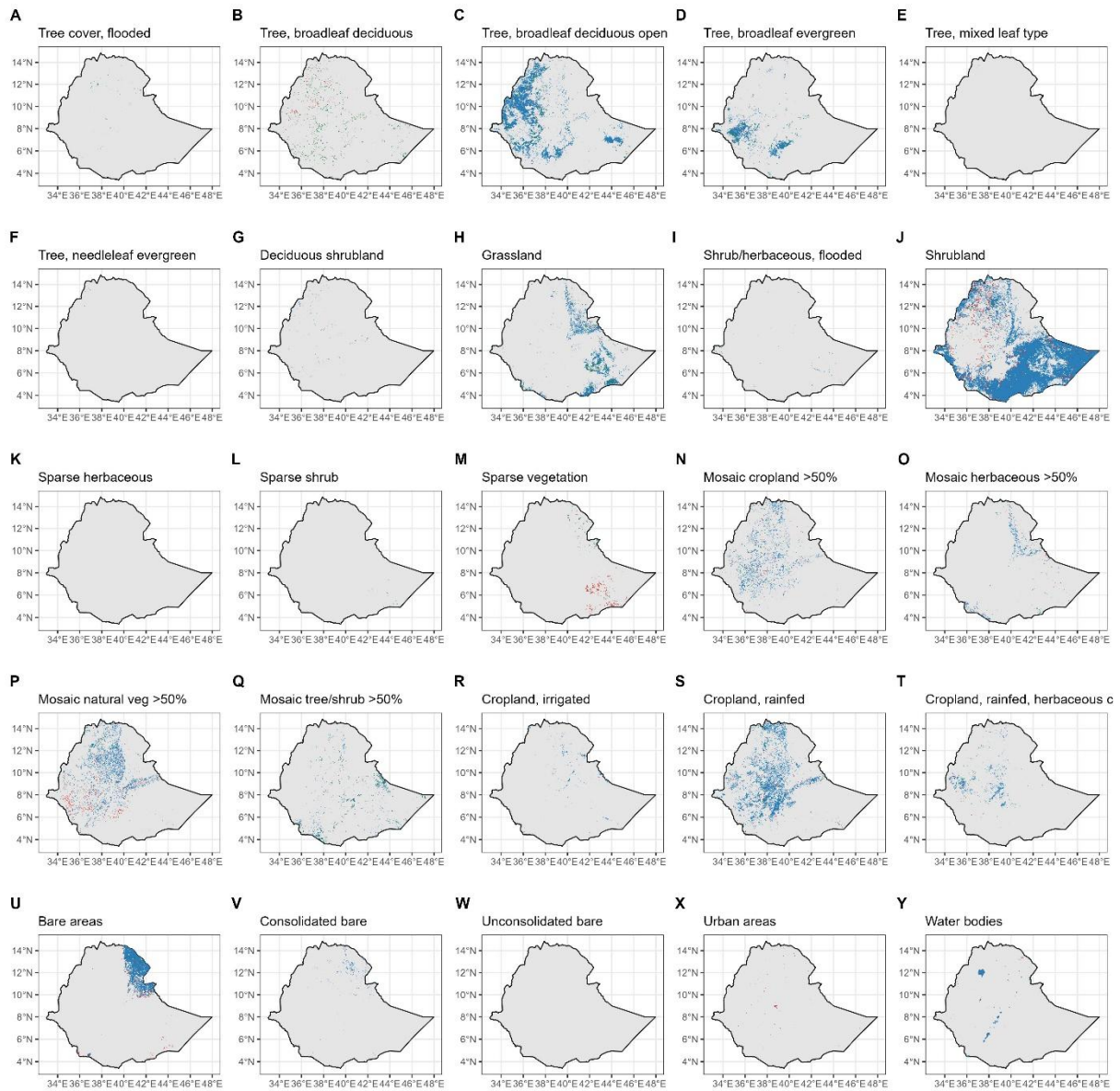
975



976

977 Figure S2. Transitions between land-cover classes from 1992 to 2020. Cell colours represent log₁₀-transformed
 978 area of transitions between land-cover classes, with darker colours indicating larger areas. Names on the axes
 979 refer to the ESA-CCI land-cover classes occurring in Ethiopia.

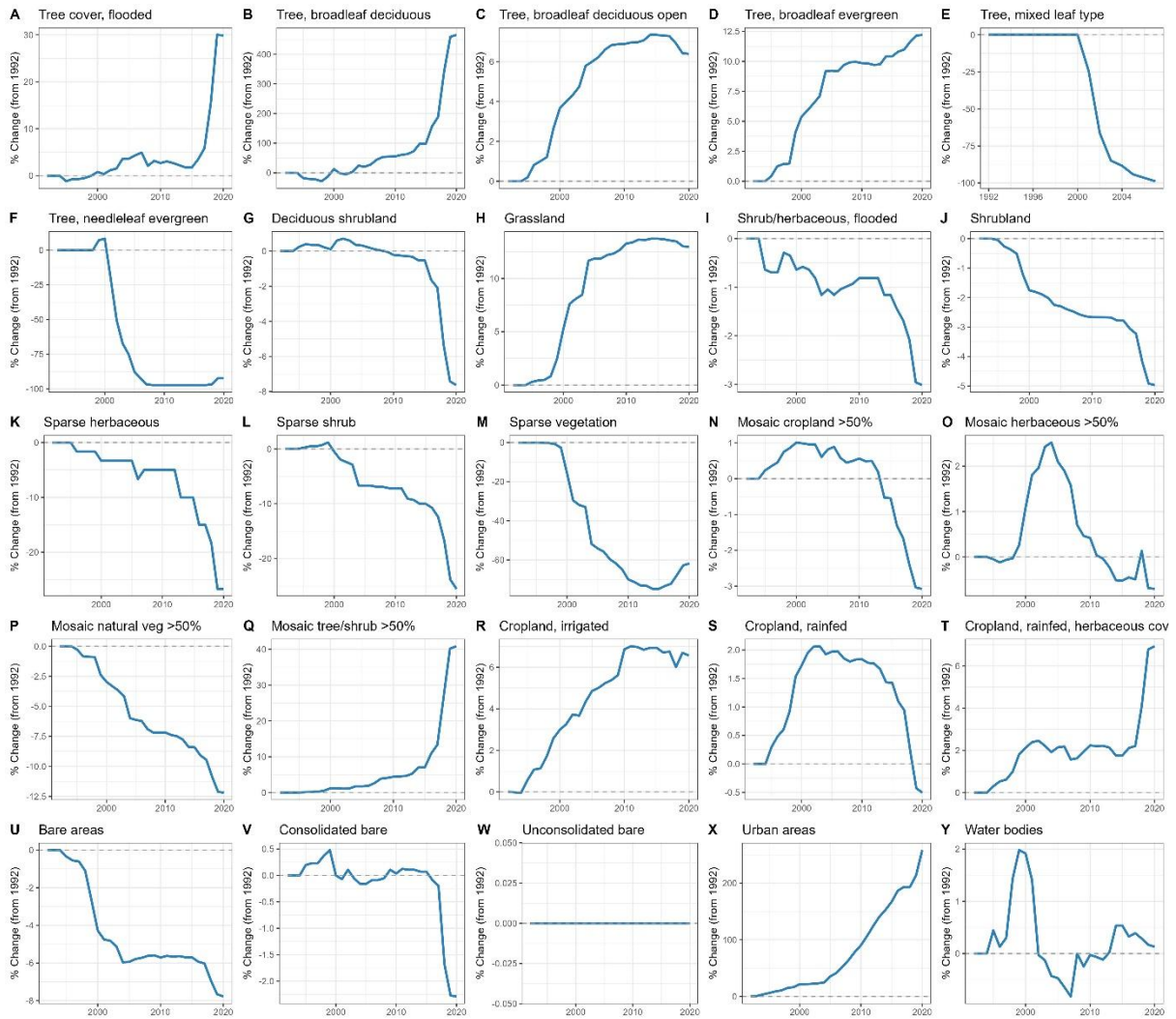
980



981

982 Figure S3. Spatial patterns of land-cover class change from 1992 to 2020. In all panels, grey represents stable
 983 absence, blue stable areas presence, red loss, and green gain in each land-cover class.

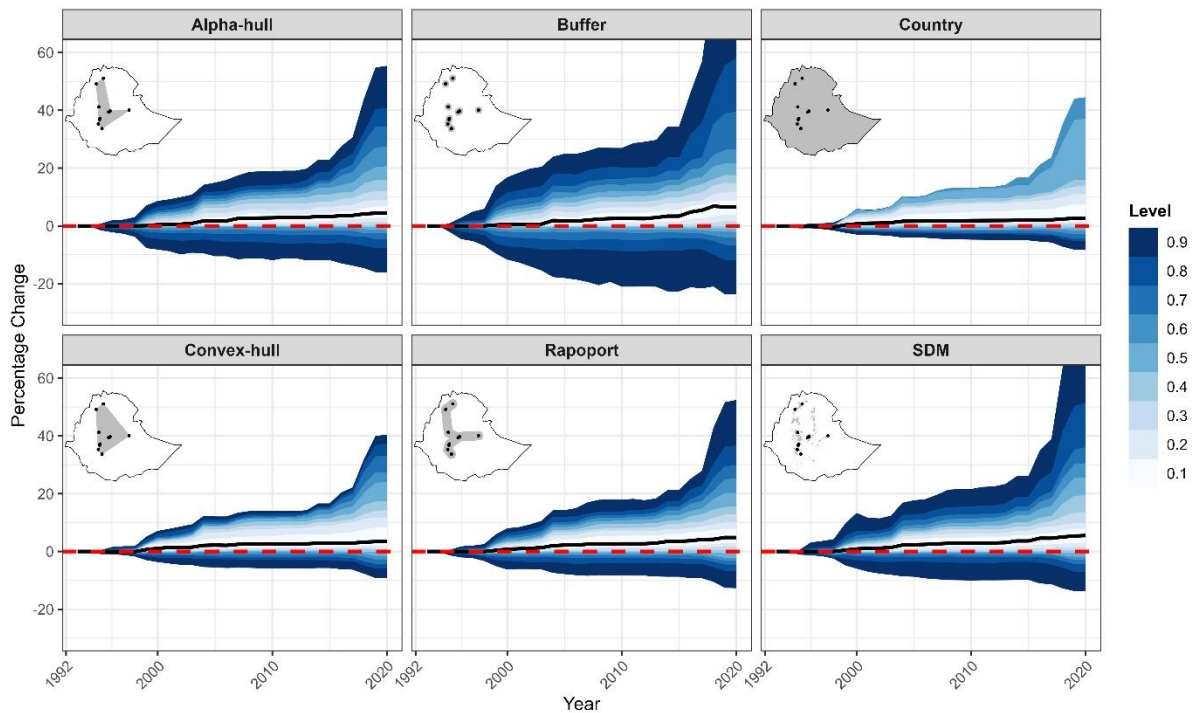
984



985

986 Figure S4. Temporal trends in land-cover class change from 1992 to 2020. Values in the y axis represent the
 987 percentage change in land-cover relative to the 1992 baseline year.

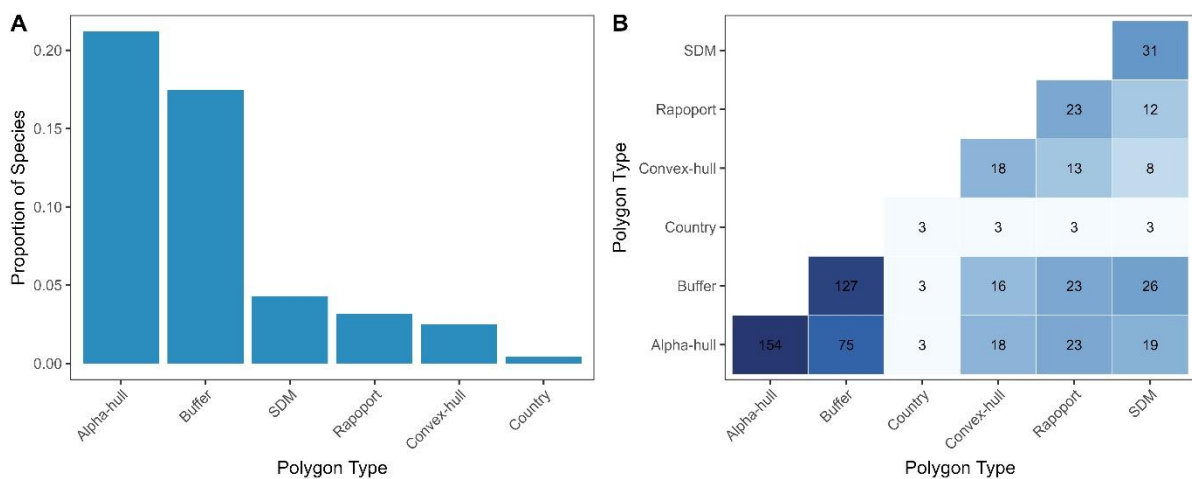
988



989

990 Figure S5. Summary of SHI for Ethiopian species under six range-mapping methods. Coloured ribbons represent
 991 the proportion of species within a particular 10%-interval class. The black line indicates the median SHI change
 992 across species.

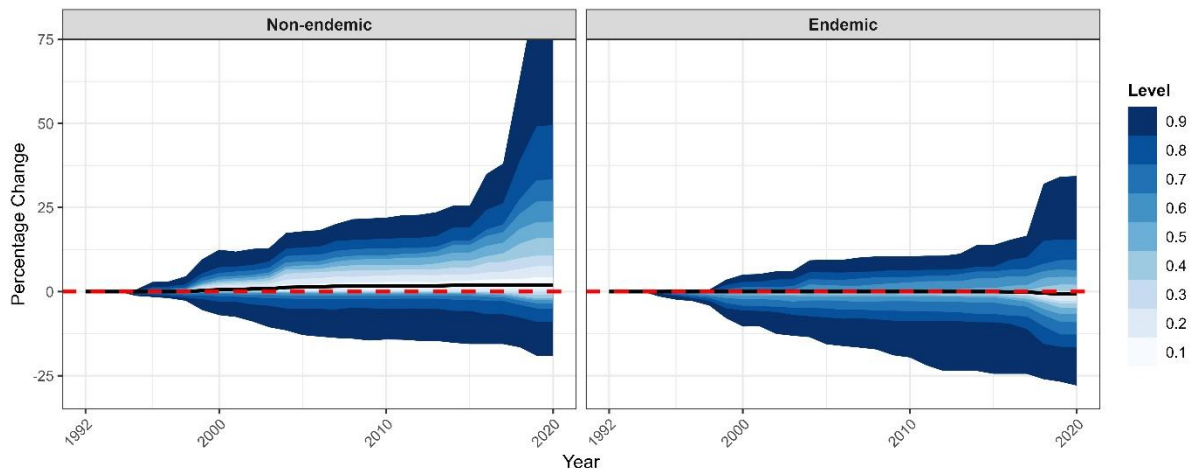
993



994

995 Figure S6. Frequency and overlap of species lacking valid AOH across range-mapping methods. (A) Proportion of
 996 species (total species = 727) without AOH in 1992 by method. (B) Shared occurrence of invalid AOH across range-
 997 mapping methods.

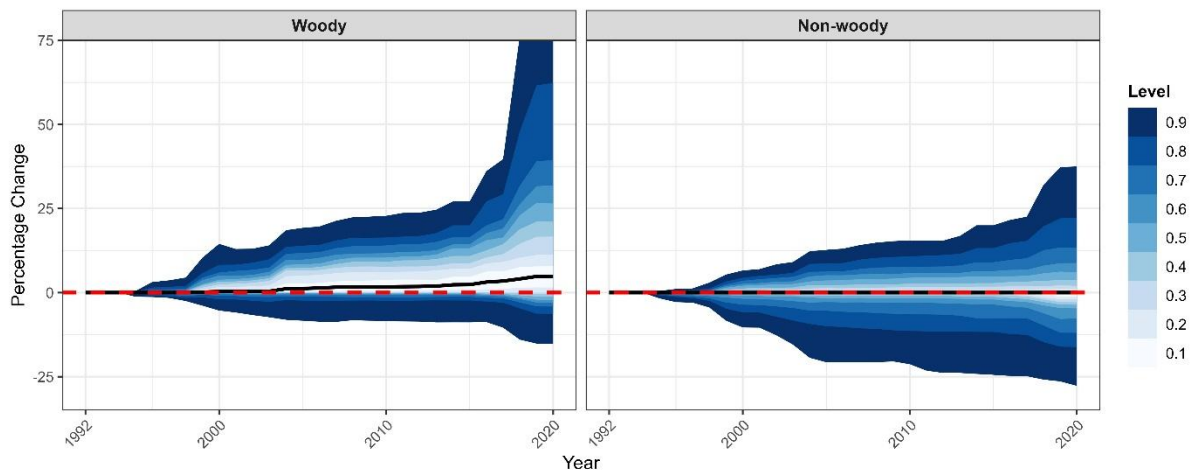
998



999

1000 Figure S7. Summary of SHI changes for endemic and non-endemic Ethiopian species. Coloured bands represent
 1001 the proportion of species within a particular 10%-interval class. The black line indicates the median SHI change
 1002 across species.

1003



1004

1005 Figure S8. Summary of SHI change for woody and non-woody Ethiopian species. Coloured bands represent the
 1006 proportion of species within a particular 10%-interval class. The black line indicates the median SHI change across
 1007 species.

1008